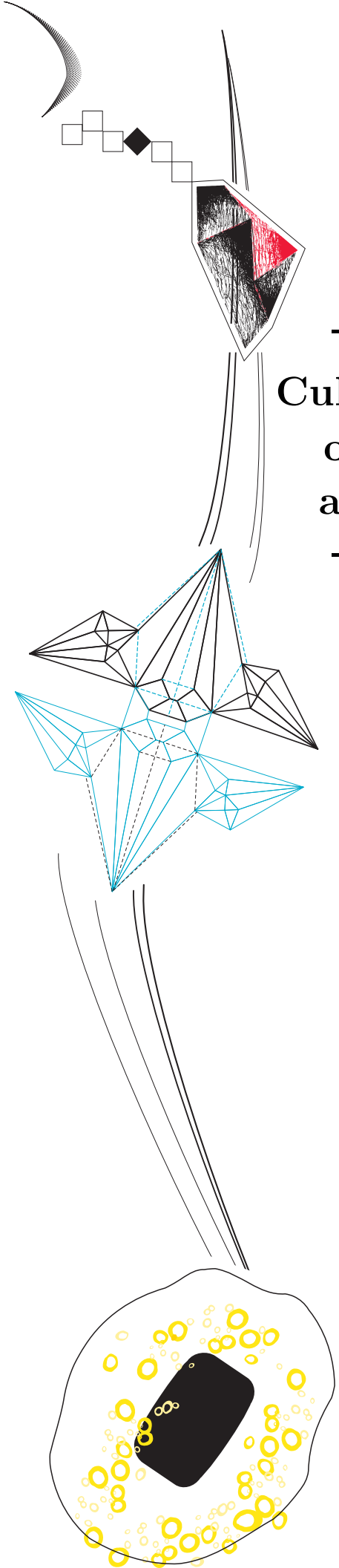

Master thesis

Faculty of Science and Technology

Culturing DRRAGN cardiomyocytes on GelTA and GelTA-MWCNT to assess differences in maturity level

Author and committee members:

Author
A.M.S. Stoter

Supervisors
Applied Stem Cell Technology
Prof. dr. Robert Passier
Developmental BioEngineering
Dr. Jeroen Leijten
External committee member
Biomechanical Engineering
Dr. ir Jeroen Rouwkema

Submitted on July 19, 2019

UNIVERSITY OF TWENTE.

Abstract

Background: A model of *in vitro* cultured mature cardiomyocytes is essential to fabricate disease models and research drug responses. Over the past years, research has been done into the use of gelatin based hydrogel scaffolds for the culturing of cardiomyocytes. However, pristine gelatin based hydrogel scaffolds lack conductivity, which is present in human cardiac tissue. Here, a method to fabricate a conductive gelatin based hydrogel scaffold is discussed.
Method: Gelatin tyramine has been mixed with multi-walled carbon nanotubes to achieve a higher conductivity of the hydrogel. To investigate the effect of the multi-walled carbon nanotubes on the conductivity of the hydrogel, a conductivity measurement is done with a four point probe. To investigate the effect of the multi-walled carbon nanotubes on the maturity of the cardiomyocytes, the RNA expression of the gene encoding connexin 43 is measured with qPCR and the expression of the connexin 43 protein is imaged with immunostaining. The orientation of α-actinine strands has also been investigated.
Results and discussion: It has been found that the presence of multi-walled carbon nanotubes did not show a positive correlation to the conductivity of the scaffolds. It is expected that this is due to the lack of a network formed by the multi-walled carbon nanotubes, causing the formation of electrical double layers at the interfaces between the carbon nanotubes and the gel. With regard to the effect of the presence of carbon nanotubes on the maturity of the cultured cardiomyocytes it is hard to draw a concrete conclusion due to the fashion in which the cardiomyocytes are cultured, as multiple cardiomyocytes are present on top of each other.
Conclusion and recommendations: During the scope of this master thesis, a design for the fabrication of thin gelatine based hydrogel layers has been optimized. For further optimization it is recommended to apply an electric field over the hydrogels with carbon nanotubes during the curing of the hydrogels, to allow the carbon nanotubes to align. This would form a network of carbon nanotubes in the gel, causing less electrical double layers to be formed.

For the fabrication of the thin hydrogel layers it is recommended to use a PMMA mold for reproducibility.

Preface

During my bachelor Technical Medicine, I found out that contrary to my expectations, I prefer to work in laboratories than with patients, so for my master I decided to switch to BioMedical Engineering, a decision I never regretted. During the course Tissue Engineering I worked with cardiomyocytes, and instantly fell in love. I decided to pursue this passion during my internship at the UniversitätsKlinikum Hamburg-Eppendorf, where I worked with engineered heart tissue. As I have also always been interested in chemistry, I wanted to incorporate this into my master thesis. When I heard about the possibility to work with both the AST and DBE group and combine my passion for cardiomyocytes with a more chemistry related subject, I could not let this opportunity pass and I am proud to present the findings and conclusions of this 45 ECTS master thesis project in this report.

Acknowledgments

There are a few people I would like to thank for their help during my master thesis. First of all I would like to thank my supervisors, Robert Passier and Jeroen Leijten, for making it possible for me to work on my master thesis in both the Applied Stem cell Technologies and Developmental BioEngineering groups. I want to thank Barbara Zoetebier for helping me find my way in the chemistry labs. I want to thank Jeroen Rouwkema for being a part of my examination committee. I sincerely want to thank Rolf Slaats for differentiating the DRRAGN cell line for me every week and Stefan Hoogland for differentiating extra COUP cardiomyocytes for me to practice with. I want to thank Douwe de Bruijn from the BIOS group for all his help, without you I would not have been able to perform the four point probe measurements. I want to thank Malin Becker for making GelTA for me and Hans de Boer for developing the four-point probe set-up. I want to thank my office buddies, Laura de Heus and every other member of both groups for all the encouragement and insights I needed an not unimportant, for making this time the great time that it was. Last but not least, I want to thank everyone else who had to put up with me the last few months and made sure I still had something to smile about through all the stress.

Contents

Chapter 1

Introduction

Even with extensive research being done on a day to day basis, cardiovascular diseases (CVD) still rank as the number one cause of death in developed countries. [1] The absence of a satisfactory human cardiovascular model prevents a lot of new drugs from reaching the market, as they cannot make it past the clinical phase. In 2011 the drug succes rate was only 5.7%. [2]

One of the steps to assess whether a drug can go on the market, is drug testing on animal models. Though animal models have a lot of advantages, such as the ability to look at the reaction of the complete organ system on drug testing, species-to-species variations make for the possibility of unreliable outcomes from animal tests. For this reason it is important to use other methods, more species related, to either replace or be combined with animal testing. Replace would be desirable due to the high costs and labor intensity that accompany animal testing, not to mention the ethical issues accompanying animal testing.

To make this replacement a reality a lot of research has been going into the use of the *in vitro* culturing of cardiac tissue with the aim of creating a reliable, reproducible model of the human cardiovascular system. The focus in this master thesis will solely be on culturing cardiac tissue and will sidestep the vascular system, though not without recognizing the importance of incorporating the cardiac tissue with a vascular system in the future. Cardiac tissue is made up of cardiomyocytes (CM). CM are cultured on scaffolds, in order to regulate their growth. Commonly used scaffolds are hydrogels, which are hydrophilic polymeric materials. Amongst other things, the Young's modulus and porosity of hydrogels can be tailored mimic the *in vivo* environment of the cells cultured on the hydrogel scaffolds.

For cardiac functions, a lot of research has recently been on the use of gelatin, which is denatured collagen, bound to methacrylic anhydride, called GelMA. In combination with a photoinitiator, oxygen free radicals are created, which cause the chain polymerisation of the methacryloyl groups. This causes new covalent bonds to form between the polymer chains, crosslinking the material. [3]

A present major drawback of using hydrogel scaffolds as basis for the culturing of CM is that cardiomyocytes cultured on these hydrogel scaffolds remain fetal, whereas the cardiomyocytes in the human heart are more mature. Differences between fetal and mature cardiomyocytes lie mainly in the contraction velocity, contraction force and morphology. [4] Due to these differences, the CM cultured on hydrogel scaffolds do not accurately mimic *in vivo* CM. To develop a cardiac model for the assessment of drug responses, it is important that the model is an accurate depiction of *in vivo* cardiac tissue, for which CM are needed which accurately mimic *in vivo* CM.

Hydrogel conductivity

The main function of the human heart is contracting, in order to pump blood through the body. These contractions are well organized in the heart. When the atria are filled with blood, the sinoatrial node, located in the wall of the right atrium, creates an excitation signal. This signal spreads through the atria, causing them to contract, pumping the blood out of the atria and into the ventricles. The electrical signal travels further, towards the atrioventricular node, which delays this signal after which it is conducted

towards the bundle of His. Together with Purkinje fibers, which are present in the inner ventricular walls of the heart, the bundle of His transports the signal through the ventricles, causing these to contract as well, pumping the blood out of the ventricles and into the pulmonary artery and aorta.

Besides the electrically conductive purkinje fibers, cardiac tissue itself also has a conductivity of around 0.1 S/m. [5] This is necessary to accurately convey the electrical signal throughout the heart. By mimicking the conductivity of the cardiac tissue in hydrogel scaffolds, the in vivo cardiac environment is mimicked more accurately. This could theoretically result in a better maturation of CM cultured on these conductive hydrogel scaffolds.

There are multiple ways to achieve a higher conductivity of hydrogel scaffolds. One way is by incorporating conductive material within the hydrogel. There are multiple materials that can be used for this, one of which are multi-walled carbon nanotubes (MWCNTs). Carbon nanotubes are rolled up sheets of carbon atoms which are chemically bonded with an extremely strong molecular interaction. Multi-walled carbon nanotubes are multiple carbon nanotube sheets within each other. One carbon nanotube has a diameter of less than 1 nm, whereas multi-walled carbon nanotubes can have diameters ranging to over 100 nm.

GelMA-SWCNT

Single walled carbon nanotubes (SWCNTs) have been used to improve the conductivity of GelMA by a reserach facility in Harvard Medical School. This research compared the incorporation of multiple concentrations of single-walled carbon nanotubes with 5% GelMA (GelMA-SWCNT) to pristine 5% GelMA on multiple fronts, also regarding the maturity of cardiomyocytes.

This research has found that increasing the mg/mL of carbon nanotubes within the GelMA, till a certain threshold, increases the Young's modulus of the GelMA. More importantly, they found that the impedance of the gel is significantly lower in the GelMA-SWCNT than in pristine GelMA. The effect of this lowered impedance on the maturity of neonatal rat cardiomyocytes was also discussed.

They showed that the cardiomyocytes adhered better to the GelMA-SWCNT than on pristine GelMA. This is in correspondence with the cell viability, which according to the researchers, increased with an increase in carbon nanotubes in the GelMA. Troponin I, which is involved in contraction and muscle calcium binding, was proven to have an increase in cardiomyocytes cultured on GelMA-SWCNT. It was also shown that the sarcomeric structures in the cardiomyocytes were better defined, elongated and more interconnected. There was no significant increase in the expression of connexin 43, which is a component of gap junctions and therefore responsible for cell-cell electrical coupling, however, it is believed that the proven more homogenous distribution of the connexin 43 benefits the cell-cell coupling.

These results all seem to be very promising, making them the basis for this master thesis. However, during the course of this master thesis it was found that the presence of MWCNTs disturbed the curing of the GelMA. For this reason it was decided to switch to gelatin tyramine (GelTA), which still cures with MWCNTs present.

In this master thesis, human cardiomyocytes were cultured both on pristine GelMA and on pristine GelTA, gelatin tyramine and on GelMA/GelTA mixed with multi-walled carbon nanotubes (MWCNT). An attempt at creating a 3D cardiac model will also be discussed. Both the effect of the incorporation of MWCNT on the maturity of the cardiomyocytes as the effect on the gel characteristics will be discussed.

1.1 Report structure

The set up of this report will now be shortly explained. In the theory chapter, the theory and background behind the important aspects of this research, most of which have just been mentioned, will be explained more thoroughly. In chapter 3, the initial concept for the fabrication of GelMA(-MWCNT) hydrogel

scaffolds will be discussed. In the same chapter, experiments done to validate these hydrogel scaffolds will also be discussed. The chapter ends with an improved concept for the fabrication of hydrogel scaffolds, based on the validation experiments. The chapter on experimental methods goes through each experiment performed to analyze both the hydrogel scaffolds and the cardiomyocytes grown on these hydrogel scaffolds. Per experiment, there will first be a short introduction to explain the goal of the experiment, including if necessary some theory behind it, after which the methods relating the experiment are discussed. The results of these experiments and the discussions of these results are given in chapter 5. A conclusion is drawn in the next chapter. The final chapter is about possibilities for future research to improve on the research discussed here.

Chapter 2

Theory

As stated, in this chapter the theory and background behind the important aspects of this research will be thoroughly explained. First of, hydrogels will be discussed, after which different subjects having to do with cardiomyocytes will be explained.

2.1 Hydrogels

2.1.1 Introduction

Hydrogels are hydrophilic polymeric materials. They are often used as scaffolds for tissue engineering due to their tunability, cell-friendly environment and suitable structural and mechanical properties. These properties are suitable as they are similar to the extracellular matrix (ECM) and allow for biochemical and signaling cell interactions.[6]

2.1.2 GelMA

Collagen is the main protein of the extracellular matrix. As denatured collagen, gelatin is a low cost biocompatible polymer, which can be used as the basis for a scaffold for tissue engineering. Gelatin is more soluble than collagen, making it easier to handle.

To tune the mechanical characteristics, Methacrylic Anhydride (MA) can be bound to the gelatin polymer strands, creating a hydrogel (GelMA) which, upon addition of a photoinitiator, can crosslink under UV radiation. Under the UV light, oxygen free radicals are created, causing the chain polymerization of the GelMA chains, crosslinking the hydrogel. This process is shown in Figure 2.1. The crosslinking proces can be performed at mild conditions, such as room temperature at a neutral pH, making it possible to control the reaction. The spatial and temporal conditions of the hydrogel can therefore be determined, which allows for the fabrication of desired pattern, making GelMA an ideal scaffold for tissue engineering. [7] [3]

The Young's modulus of pristine 10% GelMA has been measured to be 33.5 +/- 6.7 kPa. [9]

The porosity of GelMA is highly dependent on the degree of substitution of MA and the percentage of GelMA. With a degree of substitution of 57%, it has been shown that the porosity is 60% with 10% GelMA and 80% with 5% GelMA. The pore size has been researched to range between 160 and 400 μm with 10% GelMA and between 240 and 400 μm with 5% GelMA. [10] [11]

2.1.3 GelTA

Gelatin-tyramine is very similar to GelMA, as it is also based on gelatin. GelTA however crosslinks by a different mechanism, being enzymatic cross linking. The coupling of the gelatin polymer to tyramine can

be seen in Figure 2.2 (a). The enzyme Horse Radish Peroxidase (HRP) catalyzes the oxidative coupling of the tyramine groups (specifically the phenol groups) bound to the gelatin in GelTA, as can be seen in Figure 2.2 (b). The reaction is activated by the presence of H_2O_2, which functions as the oxidant. The time in which the GelTA solidifies can be regulated by the HRP concentration and can differ between a few seconds to multiple minutes. Similar as with GelMA, with GelTA the crosslinking proces can be performed at mild conditions, such as room temperature at a neutral pH, making it possible to control the reaction. The spatial and temporal conditions of the hydrogel can therefore be determined, which allows for the fabrication of desired pattern, making GelTA an ideal scaffold for tissue engineering. However, as H_2O_2 is toxic to cells, it has to be determined how much the viability of the CM is dependent on the low concentration of the H_2O_2. [12] [13] [14]

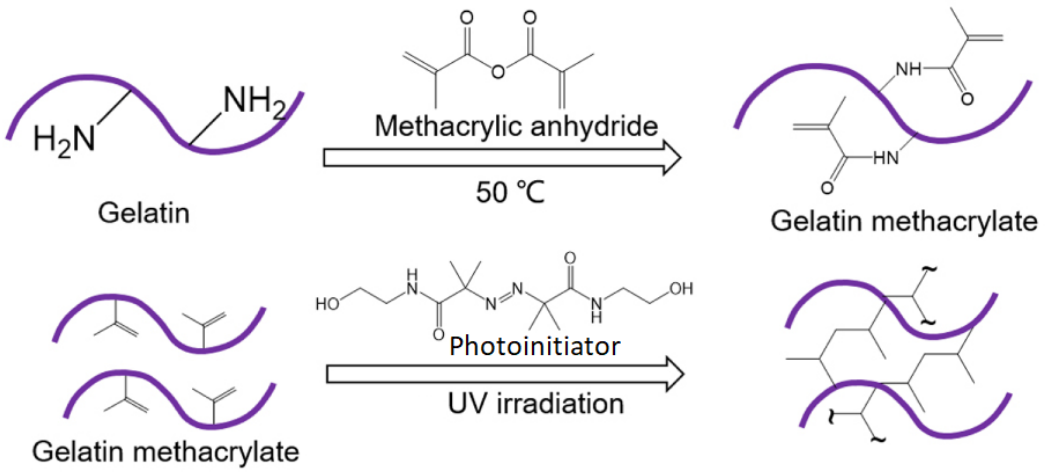

Figure 2.1: **Photoinitiated crosslinking of GelMA strands**. Figure adapted from [8].

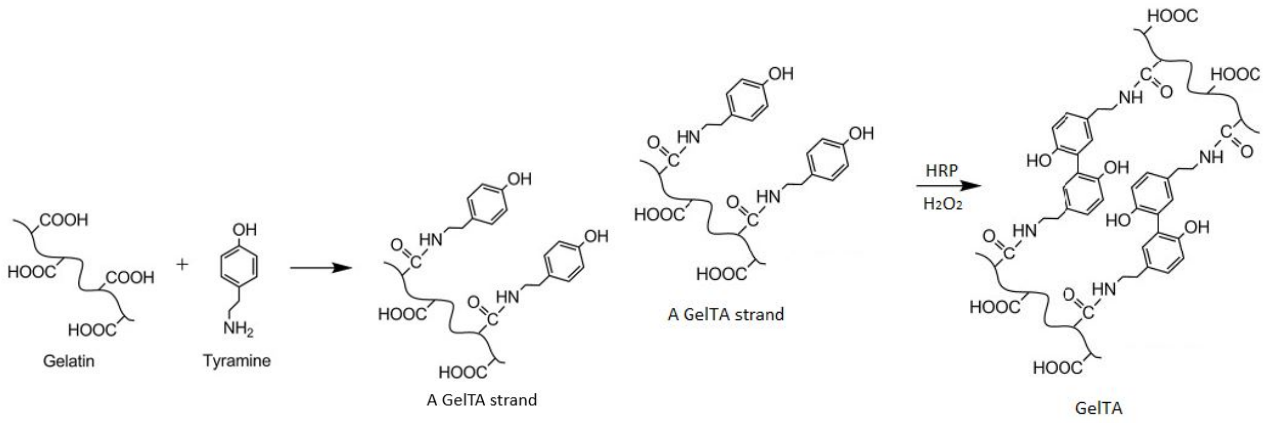

(a) (b)

Figure 2.2: **Formation and crosslinking of GelTA**. In (a) the formation of GelTA strands is shown. In (b) the crosslinking of these GelTA strands is seen under the influence of HRP and H_2O_2. Figures adapted from [15].

2.1.4 Poly(ethylene) oxide

Migration of CM through a 3D cardiac model can be improved by using a 3D model with an interconnected porous network at μm level. This environment can be created based on an aqueous two-phase emulsion of biocompatible solutions, that do not blend well, being GelMA or GelTA and poly(ethylene) oxide (PEO). These solutions mix, but due to the low interfacial energy between GelMA and PEO, the solutions will separate over time. The rate of the separation is dependent among other things on temperature and ratio of GelMA:PEO. Due to this, the solutions can be mixed together and the GelMA or GelTA can be crosslinked, after which the PEO can leach out. This leaves behind a porous, interconnected network. The porosity of this 3D model is tunable, depending on the amount and size (in kDa) of PEO. As the structural integrity is dependent on the pore size, an optimal should be found between a porosity that stimulates cell migration, but a structural integrity similar to cardiac tissue to promote maturation. It has been researched that with GelMA:PEO, the optimal ratio was 1:1, with a GelTA end percentage of 5 and a PEO percentage of 1.6 for different cell types, including human hepatocellular carcinoma cells and human umbilical vein endothelial cells. This research has to the best of my knowledge not yet been performed with CM. [7]

2.2 Conductivity of hydrogels

As described in the introduction, cardiac tissue is conductive. Therefore using conductive hydrogels to accurately mimic *in vivo* cardiac tissue could increase the maturity of the CM cultured on the conductive scaffold.

Intrinsically conductive hydrogels exist, such as polypyrrole, a polymer made up of the building block the pyrrole monomer. As pure polypyrrole is can be brittle, it can be difficult to process. It has been found that a polypyrrole blend with another material can come as a solution. This solution has been found in the polypyrrole-alginate blend. Alginate is more often used as a synthetic extracellular matrix, making it suitable for tissue engineering. [16] Independent on the ratio of polypyrrole and alginate, the conductivity of the hydrogel is 1 S/m, whereas the conductivity of myocardium is 0.13 - 0.16 S/m. [5] [17]

So there is a factor 10 difference in conductivity between the polypyrrole-alginate hydrogel and native myocardium, implying the need for a hydrogel with a conductivity more closely related to native myocardium.

A blend of polypyrrole with chitosan has been found to have a conductivity slightly lower than that of native myocardium, but in the same order of magnitude. Though the results from using a polypyrrole-chitosan blend for injection on *in vivo* post-myocardial infarction scar tissue are very promising, finding a different hydrogel with the same conductivity as native myocardium is still worth researching.

A different method to obtain electrically conductive hydrogels is mixing intrinsically non-conductive hydrogels with conductive material. A common used conductive nanomaterial due to their inert nature, making it biocompatible, is gold nanoparticles. The cardiac differentiation of mesenchymal stem cells has been shown to improve in cells cultured on a chitosan scaffold blended with gold nanoparticles. [5] It has also been found that electrical waves reproduce faster through hydrogel incorporated with gold nanoparticles than without incorporation of gold nanoparticles. [18]

However, up to 70% of gold nanoparticles are accumulated in the liver. As the idea behind using a scaffold for *in vivo* use is the degradation of the scaffold, the incorporated nanoparticles would be released throughout the body and accumulate in the liver, possibly having a cytotoxic effect. [19] [20]

2.2.1 MWNCT

A different material to blend through the hydrogels is carbon nanotubes. Carbon nanotubes are rolled up sheets of carbon atoms which are chemically bonded to have an extremely strong molecular interaction. Multi-walled carbon nanotubes (MWCNTs) are multiple sheets of bonded carbon atoms rolled over each other, whereas a single-walled carbon nanotubes (SWCNTs) is one rolled up sheet of carbon atoms. A SWCNT has a diameter of less than 1 nm, whereas MWCNTs can have diameters ranging to over 100 nm, depending on the amount of walls. As described in the introduction, a research with SWCNTs has been performed by Su Ryon Shin, 2013, with promising results. [21] Though there is still a lot of doubt regarding the subject, some researches have found that SWCNTs induce more apoptosis than MWCNTs due to their small surface area and hydrophobic nature. It is also believed that due to their size, SWCNTs are more likely to puncture cell membranes. However, it has been found that both CNTs cause an increase in inflammation and oxidative stress due to accumulation in cardiac tissue.

The functionalization of MWCNTs can also influence the toxicity. To the best of my knowledge, the toxicity of MWCNTs with a GelTA coating has not yet been researched.

In conclusion, handling MWCNTs should therefore be done with great care and possible benefits of an increase in maturity have to be compared to possible toxicity risks. [22] [23] [24]

How to measure the conductivity of the hydrogel will be discussed in the experimental chapter.

2.3 Culturing Cardiomyocytes

Cardiomyocytes are rod-shaped cells and the main cells present in cardiac tissue. CM contain myofibrillar structures, including sarcomeric bands, which consist of the contractile proteins actin and myosin. Sarcomeric bands are necessary for the contraction of CMs. [25] [26] [27]

There are different types of CMs, being pace maker cells (or nodal cells), atrial and ventricular. Nodal CMs are located in the sinoatrial node in the heart, which generates an excitation pulse. Adjoining CMs spread this excitation pulse along the plasma membrane, through the heart, causing first the atria to contract. After a slight delay, the ventricles follow, which regulates the flow of oxygen rich blood through the body. On average, the rest frequency of these contractions are 1-1.5 Hz. [28] [29]

When the excitation pulse travels across the adjoining CMs, each individual CM it comes into contact with, contracts too. The mechanism behind this is as follows; When the excitation pulse travels across the membrane, it comes into contact with the sarcoplasmic reticulum, located on the membrane. This stimulates an exchange of Ca^{2+}, Na^{+} and K^{+} in voltage gated ion channels, causing the membrane potential of the CM to depolarize from negative to positive. Due to the Ca2+ exchange, there is an increase of Ca^{2+} in the CM, which causes myosin to bind to actin. This is the start of the contraction. After the contraction there is a repolarization phase in which the myosin and actin release each other and the CM relaxes. Electrical and mechanical characteristics of the CMs are harmonized by intercalated disks that join neighbouring CMs. [30] The contraction characteristics are dependent on the type of CM as ventricular CMs generally contract with greater force, to put more force behind the blood flow, as it has to travel across a greater distance. [31] [32] [33] [34]

2.3.1 Medium

To ensure the cultured CM have enough nutrients for their survival, their medium supply is refreshed twice a week. The nutrients are present in nutrient rich, serum-free cardiomyocyte medium, with some additions to promote the maturation of the CM.

The first addition is the thyroid hormone triiodothyronine (T3). It has been found that T3 promotes maturation of calcium handling, which is responsible for contraction characteristics. CM cultured with

T3 supplements are found to have an increase in cell size and sarcomere length, both associated with a mature phenotype. T3 supplementation has also been found to causes a more mature phenotype based on action potentials characterisics. T3 is added to the cardiomyocyte medium in a 1:30 ratio. [35] [36]

The second addition is Insuline-like Growth Factor (IGF-1). It has been found that IGF-1 in an *in vivo* heart regulates among other things the contractility of the heart, which is an important maturation marker. IGF-1 is added in a 1:1000 ratio. [37]

To make up for the increase in pH of the medium due to the addition of T3, HCl is added in a 1:100 ratio.

2.3.2 DRRAGN

The specific cell line that will be used for the experiments performed in this master thesis, is called the Double Reporter mRubyII Actinine GFP Nkx2.5 cell line, or in short the DRRAGN cell line. As the name suggests, this cell line is manipulated to have a double fluorescent reporter, both for the α-actinine, which has been labeled with mRubyII and thereby helps visualize the orientation of the sarcomeres in the CM, and for green fluorescent protein (GFP), bound to Nkx2.5, which is a marker for cardiomyocyte differentiation. Due to this a Fluorescence Activated Cell Sorter, can in a cell suspension analyze the percentages of cardiomyocytes (GFP (and therefore Nkx2.5) positive and α-actinine positive), cardiac pacemakers (GFP (and therefore Nkx2.5) negative and α-actinine positive), or other cell types.

The differentiated DRRAGN CM are both atrial and ventricular. The exact ratio between atrial and ventricular CM present in the differentiations is unknown. The DRRAGN cell line is derived from Embryonic Stem Cells.

2.3.3 Cell attachment

To be able to culture CM on top of hydrogels, it is important to understand how CM attach to this hydrogel.

Certain proteins contain RGD (arginine-glycine-aspartic acid) attachment sites, to which certain integrins serve as receptors. These integrins are transmembrane proteins, with usually a small intracellular cytoplasmic domain, a part that spans the membrane and a large extracellular domain.

The proteins containing the RGD attachment sites are present in the cell suspension medium and bind to the hydrogel. As the proteins have bound to the hydrogel and the CM can bind to the proteins, in effect the CM are attached to the hydrogel. The degree to which proteins adsorb to the hydrogel surface is dependent on among other the surface charge and hydrophilicity of the hydrogel surface. [38] [39] f Gelatin contains many RGD attachment sites, and as gelatin is the main component of both GelMA and GelTA, the CM should be able to attach to these hydrogels. [3]

2.3.4 3D vs 2D

As the goal is to mimic *in vivo* CM, it goes without saying that a 3D environment would be more ideal to culture CM in due to the ability for CM to have spatial migration and cell-cell contact, whereas a 2D environment only offers planar migration and cell-cell contact. [7]

2.4 Maturity

The maturation of CM has been mentioned numerous times in this report. Though it already sounds plausible that mature CM are desired, as the goal is to mimic a mature *in vivo* heart, what it exactly entails for a CM to be mature, will be explained here.

Parameters	Details	Fetal Cardiomyocytes	Mature Cardiomyocytes
Morphology	Cell shape	Circular	Rod-shaped
	Nucleus	Round	Elongated
Sarcomeres	Structure	Disarrayed	Highly organized
	Length	Around 1.6 μm	Around 2.2 μm
Multinucleation		Mononucleated	25% Multinucleated
Contractile force		nN range per cell	μN range per cell
Conduction velocity		Around 0.1 m/sec	0.3-1.0 m/sec

Table 2.1: **Fetal versus mature CM.** Different characteristics are listed which show the difference between fetal and mature CM. Table adapted from [4].

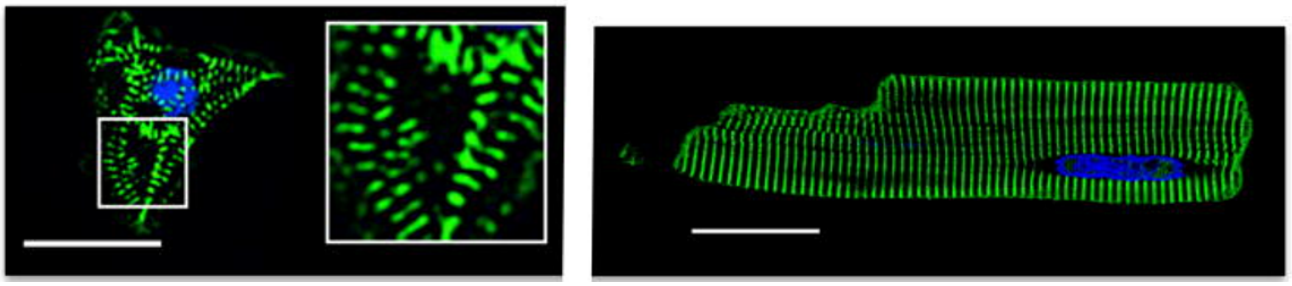

(a) (b)

Figure 2.3: **Morphology Cardiomyocytes**. In both (a) and (b) the alpha-actinine are stained with green and the nuclei with blue. (a) A fetal cardiomyocyte is shown. (b) A Mature cardiomyocyte is shown. The scale bar in (a) and (b) is 25 μm. Figures are taken from [4].

Multiple characteristics determine the difference between fetal and mature cardiomyocytes, of which the most relevant in relation to this master thesis are shown in Table 2.1. [4] The binucleation seen in mature CM usually occurs during postnatal hypertrophy of the heart. [40]

The significant differences in morphology can best be shown with Figure 2.3, with regard to size, length to width ratio, alpha-actinine orientation and length, and shape of the CM and shape of the nuclei. [4]

The individual sarcomeres in the fetal CM are less well defined and very disorganized, whereas the sarcomeres in the mature CM were clearly defined and highly organized in parallel bundles. [41]

A last characteristic for maturity important for this master thesis, is the protein Connexin 43 (Cx43). Cx43 is expressed by CMs when gap junctions are formed, which regulate the spread of current through neighbouring CMs. As the current is directly linked to the contractions of the CM, the gap junctions regulate the conduction velocity, which as mentioned is a measure of maturation. [21]

2.4.1 Characteristics to be investigated

The general cell characteristics which will be assessed are the viability of the CM, which will be assessed with a live-dead staining, and the contractility of the CM, which will be assessed with a software called MotionGui.

There are also many characteristics associated with maturity of CM as just described. Unfortunately, not all of these can be examined in the CM cultured in this master thesis. A choice has therefore been made, based on characteristics deemed most important and available resources. The goal of the experiments which are performed is to give insight into possible maturation differences related to the presence of MWCNTs in the scaffolds on which the CM are cultured.

The experiments which are performed are a qPCR, which is performed to measure the RNA expression of the gene encoding for Cx43, and an immunostaining of the CM to compare the expression of the Cx43 protein. Furthermore the alignment of sarcomeres will be compared.

How each of these experiments are performed is discussed in chapter 4.

Chapter 3

Fabrication protocol

This project started with an initial concept for a facile fabrication method of hydrogel scaffolds for culturing hiPSC-CM. To validate and improve this fabrication method, multiple experiments have been done. These experiments uncovered necessary changes to the initial fabrication method, leading to an optimized version. The path to this optimized version will be discussed, starting with 1) initial concept, followed by 2) validation of this concept and ending with 3) the optimized method.

3.1 Initial Concept

The initial concept for the fabrication of GelMA(-MWCNT) hydrogel scaffolds is based on the article by Su Ryon Shin, 2013 [21]. The researchers in this article used GelMA, into which SWCNTs were mixed. This made for the conductive GelMA-SWCNT hydrogel. The GelMA(-SWCNT) is mixed with a photoinitiator, making the GelMA strands crosslinkable under UV light. As MWCNT are more viable than SWCNT, see subsection 2.2.1, the initial fabrication protocol as described by Su Ryon Shin has been adapted to use MWCNTs instead of SWCNTs in this master thesis. The MWCNTs have been ordered from nano-lab with order number PD30L5-20-COOH. They guarantee a purity of >95%.
The first step of the facile fabrication method is to make the GelMA. An extensive protocol for this is obtained from Su Ryon Shin and can be found in section A.1 and is based on [42]. In short, 5 g gelatin is dissolved in 50 mL sodium carbonate - sodium bicarbonate buffer at 50 °C. When all the gelatin is dissolved, the pH of the solution is adjusted to 9 and 0.5 mL Methacrylic Anhydride has to be added. To stop the reaction of the gelatin with the Methacrylic Anhydride, the pH has to be readjusted to 7.4. The solution has to be dialysed to remove toxic, exces Methacrylic Anhydride for at least 5 days. After this the solution is freeze dried and ready to use.
To crosslink the GelMA hydrogel, 0.5% photoinitiator has been dissolved in a variable GelMA percentage. Su Ryon Shin, et al, 2013, used 5% GelM, which she dissolved in DPBS. The solution has been put in a warm water bath for an hour for the GelMA to fully dissolve. To prevent the MWCNT from leaking out of the hydrogel when mixing them through the GelMA, it is crucial to coat the MWCNT with GelMA to activate teh surface of the MWCNT beforehand. By mixing 20 mg MWCNT with 140 mg GelMA in 4 mL DPBS, the MWCNTs are coated with GelMA. When the coated MWCNTs are then mixed through the GelMA, the coating on the MWCNTs binds to the GelMA strands, preventing the MWCNTs from leaking out of the. To ensure a homogenous distribution of the MWCNT throughout the fluid, it has to be placed in a bath sonicator for an hour. Su Ryon Shin, et al, used a VCX 400 bath sonicator at 80 W for 2 secs on and 1 sec off, as this exact one was not available to me, the Branson 1510 Ultrasonic Cleaner has been used. On this bath sonicator it is not possible to apply the 2 sec on 1 sec off setting. This setting is used so as not to overheat the GelMA, as high temperatures affect gelatin [43]. As the temperature can be set on the Branson 1510 Ultrasonic Cleaner, this is a good solution. The temperature is set to 40 °C.

[21] When the MWCNT are homogenously dispersed, the MWCNT can be mixed through the GelMA. By adding 1:4 MWCNT stock solution:GelMA, you create a GelMA solution with 1 mg/mL MWCNT. This can of course be adapted to the desired amount. The amount of MWCNT in the MWCNT stock solution can also be upschaled. For the outcome of the GelMA concentration, it has to be taken into account that by sonicating the MWCNT solution, the GelMA strands shorten or degrade and therefore do not add to the end concentration.

GelMA can attach to glass coated with 3-(trimethoxysilyl)propyl methacrylate (TMS-PMA). [3] Su Ryon Shin, et al, used a protocol to coat the glass slides in which the TMS-PMA on top of the glass slides is placed in an 80 °C oven [21]. As placing TMS-PMA in an oven methacrylates the entire oven, we switched to another protocol in which this step was excluded. This protocol was adapted from the product information of TMS-PMA from Sigma Aldrich, with catalog number M6514.

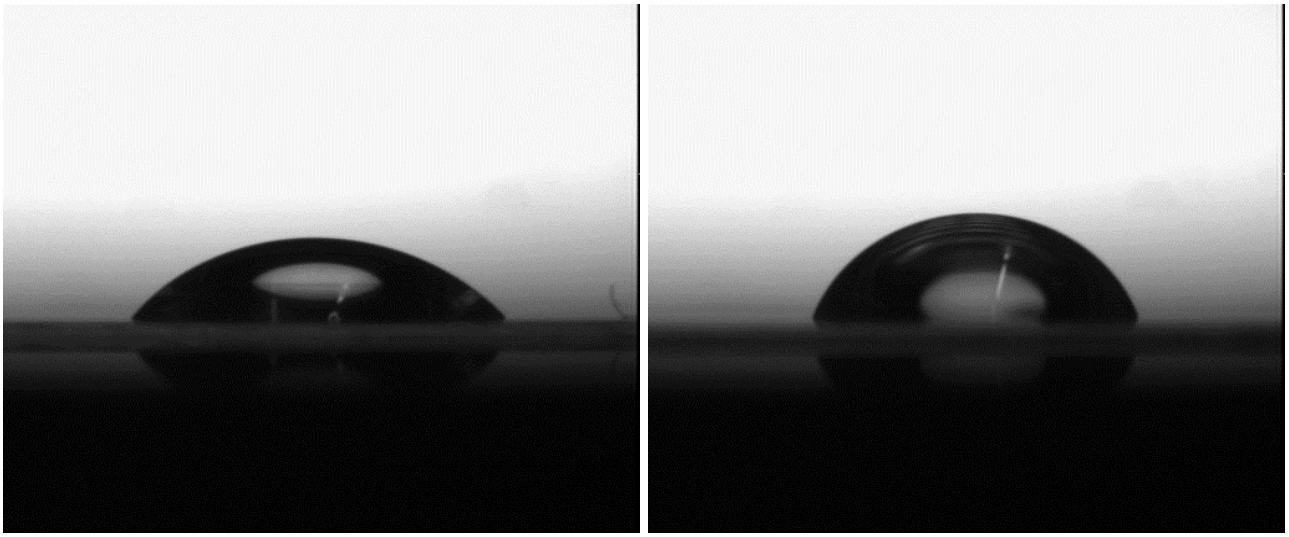

(a) (b)

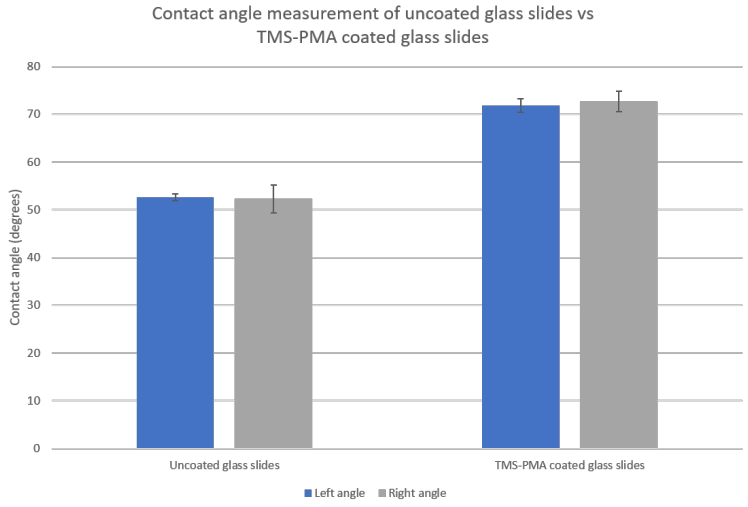

(c)

Figure 3.1: **Contact angle measurement**. (a) Representative picture of a water droplet on top of an uncoated glass slides, (b) Representative picture of a water droplet on top of a TMS-PMA coated glass slides, (c) Graph depicting the exact contact angles in degrees of the left and right side of the water droplets on top of the uncoated glass slides versus the TMS-PMA coated glass slides.

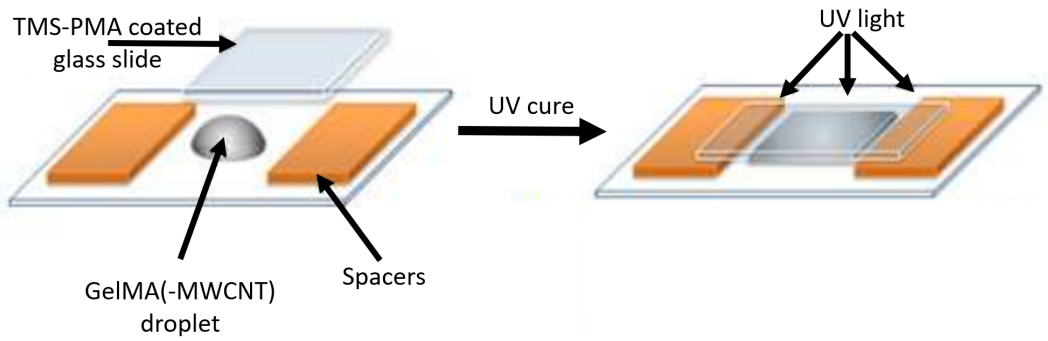

Figure 3.2: **Fabrication of thin GelMA(-MWCNT) layers**. A polymer drop is placed within spacers, being layers of scotch tape, after which the drop is flattened with a coated glass slide. UV curing causes the polymer to crosslink. Figure adapted from [21].

In this protocol, first the glass slides are thoroughly cleaned, with soap and ethanol, and dried in a drying oven. Thereafter TMS-PMA is diluted in reagent ethanol with dilute acetic acid. The cleaned glass slides are emerged in this solution. After 3 minutes the TMS-PMA should be sufficiently adhered to the glass slides and the excess TMS-PMA solution can be rinsed off the glass slides. Allow the glass slides to dry thorougly before use. To verify whether the adopted protocol works, a contact angle measurements has been done, of which the results are shown in Figure 3.1. In figure 3.1 (a) and (b) pictures are shown of the water droplets on top of the (un)coated glass slides, while (c) shows the exact contact angles, with n=3. From figure 3.1 it can be seen that the TMS-PMA coated glass slides are significantly more hydrophobe than the uncoated glass slides, showing that the adapted coating protocol was effective.
When both the glass slides are coated and the GelMA(-MWCNT) polymer solution is dissolved, the thin hydrogel layers can be fabricated. Su Ryon Shin, et al 2013, pipetted a drop of 10 μL of the GelMA(-MWCNT) solution on top of a petri dish, within two spacers, as depicted in Figure 3.2. For the spacers they used 3 layers of regular Scotch tape, creating an expected height of 50 μm. To flatten the GelMA(-MWCNT) droplet, the TMS-PMA coated glass slide is placed on top, as is shown on the left side of Figure 3.2. To crosslink the hydrogel, the petridish is then placed under an UV source with a wavelength of 360-480 nm and an intensity of 6.9 mW/cm^2. The UV exposure time is dependent on the amount of MWCNT within the polymer, being 5, 50, 80, and 120 s for 0, 1, 3, and 5 mg/mL SWCNTs, respectively. [21]

As MWCNTs will be used instead of SWCNTs, the optimal UV exposure times for this master thesis have to be determined. The UV irradiation will be done with the UV-KUB, with a max intensity of 40%.

After the GelMA(-MWCNT) thin layers have crosslinked, the layers are ready for use. The cardiomyocytes can then be cultured on top of the layers, which concludes the initial concept.

3.2 Fabrication validation and improvements

The validation of the discussed initial fabrication concept for MWCNTs will now be explained, as well as the used improvements with regards to gel homogeneity, reproducibility, cross-linking and a 3D cardiac environment.

3.2.1 Homogeneous distribution of MWCNT

When validating the MWCNT distribution throughout the GelMA at a 10x magnification, it became apparent that the distribution was not homogeneous, as is shown in Figure 3.3 (a).

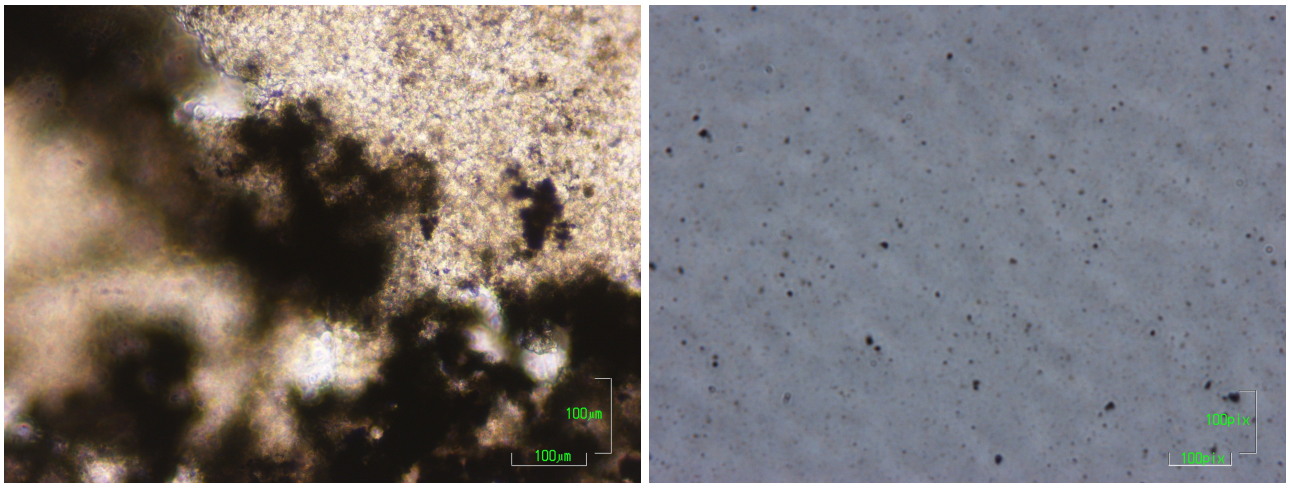

(a) (b)

Figure 3.3: **MWCNT distribution with bath vs probe sonicator**. (a) Picture of the distribution of the MWCNT throughout the GelMA after using a bath sonicator for an hour showing a not homogeneous distribution of the MWCNT, (b) Picture of the distribution of the MWCNT throughout the GelMA after using a probe sonicator for 10 minutes with a duty cycle of 60% at output 4, showing a close to homogeneous distribution of the MWCNT.

A homogeneous distribution of MWCNTs throughout the GelMA is desirable, as it is desirable for the CM cultured on the GelMA-MWCNT hydrogel to all be in contact with the same GelMA:MWCNT ratio. This is necessary to be able to say that the reaction of the CM to the hydrogel is equal across the entire hydrogel.

Leaving the MWCNT solution in the bath sonicator for longer periods of time did not affect the distribution of the MWCNT. A different method of distributing the MWCNT in the GelMA therefore had to be found. For this the Branson Ultrasonics Sonifier S-250A. As shown in Figure 3.3 (b), by inserting the probe sonicator in the MWCNT solution for 10 minutes with a duty cycle of 60%, which determines the pulse duration as a percentage of a second, and at output control 3, the distribution of MWCNT was near homogeneous. Therefore I recommend using a probe sonicator to overcome this limitation.

3.2.2 Crosslinking

To validate the crosslinking of the GelMA-MWCNT, the initial concept was followed, after which the solidity of the GelMA-MWCNT was tested, by placing it in DPBS. It was observed that the MWCNTs distribute throughout the DPBS, which means that the crosslinking of GelMA-MWCNT was not sufficient to solidify the GelMA-MWCNT.

The expected reason behind the GelMA-MWCNT not crosslinking sufficiently, is the blackness of the MWCNT, which can be seen in Figure 3.4. As this solution is very black, it is expected that a lot of the UV light is absorbed by the MWCNTs. This prevents the UV light from penetrating through the gel far enough to cure throughout the entire gel. This theory was validated by making a very thin layer of GelMA-MWCNT by placing 2 glass slides directly on top of each other, which did cure under the UV light. In other words, when the amount of GelMA-MWCNT is too much, UV light is not able to penetrate through all of the gel and can therefore not crosslink all of it, whereas a thin layer does not absorb as much light and does crosslink.

That it was not possible to cure the GelMA-MWCNT did raise the question why it did work in the research done by Su Ryon Shin [21]. This is probably because in the research by Su Ryon Shin single

Figure 3.4: **Blackness of GelMA-MWCNT**.

walled CNTs were used, whereas multi walled CNTs have been used here. The expectation is that the extra walls take up more of the UV light, limiting the penetration depth of the UV light more than with the SWCNTs. To validate this theory the same process as described here should be repeated by using SWCNTs. If 50 μm thick GelMA-MWCNT layers can be formed, this would substantiate this theory.

Different methods have been tried to be able to cure throughout the entire hydrogel layer.

- A prolonged exposure to the UV light did not improve the curing.
- Aluminum foil has been placed under the petridish on which the hydrogel layers are fabricated. The aluminum foil reflects all the UV light that passes through the mold which can then cure the GelMA-MWCNT from below. This did not sufficiently increase the curing to create a 50 μm thick layer.
- A thinner PDMS mold has been made to prevent the PDMS from absorbing too much of the UV light, which also did not sufficiently increase the curing.
- A combination of the thin mold and the aluminum foil also did not sufficiently increase the curing.
- Higher amounts of photoinitiator have been used, also in combination with the thin mold and aluminum foil under the petridish, but this also did not increase the curing enough to make a layer.
- A different method of curing has been tried, being enzymatic curing in GelTA. With GelTA, it was possible to cure throughout the entire GelTA-MWCNT layer. The fabrication of GelTA is discussed in subsection 3.2.3.

Using ruthenium and visible light to cure throughout the GelMA-MWCNT has also been considered, but the expectation is that when UV light cannot penetrate the GelMA-MWCNT deep enough to crosslink the entire gel, neither will visible light.

3.2.3 GelTA

Due to all mentioned limitations with the crosslinking of GelMA, it was decided to switch to another gelatin based hydrogel, which uses a different method of crosslinking, namely GelTA. GelTA crosslinks enzymatically, which should not be affected by the presence of MWCNT.

As I did not make GelTA, an extensive protocol is not made available in this report. The GelTA was produced for me by Malin Becker. First 5 g gelatin was dissolved in MiliQ, after which 3.46 g DMTMM and 2.17 g TA HCl was added thrice over consecutive days. At day 4 50 g NaCl was added together with cold EtOH to start the precipitation of the GelTA. After the GelTA is precipitated, the EtOH is poured out and the precipitation left to dry by air. After it has completely dried, the precipitation is taken out of the flask and resuspended in MiliQ. Similar to with GelMA, the GelTA is then dialyzed for 5 days and freeze dried, after which the finished GelTA product is obtained. The expected yield of the transformation of gelatin to GelMA was 50%, it was however closer to 20%. It is therefore advisable to search for a different method of GelTA production with a higher yield. For the GelTA to be able to crosslink, it has to be mixed with HorseRadish Peroxidase (HRP) at 40 units/mL. The amount of HRP mixed through the GelTA determines the speed of the crosslinking. The mixing of the MWCNT through the GelTA is the same as with the GelMA, first the MWCNT are coated with GelTA after which they

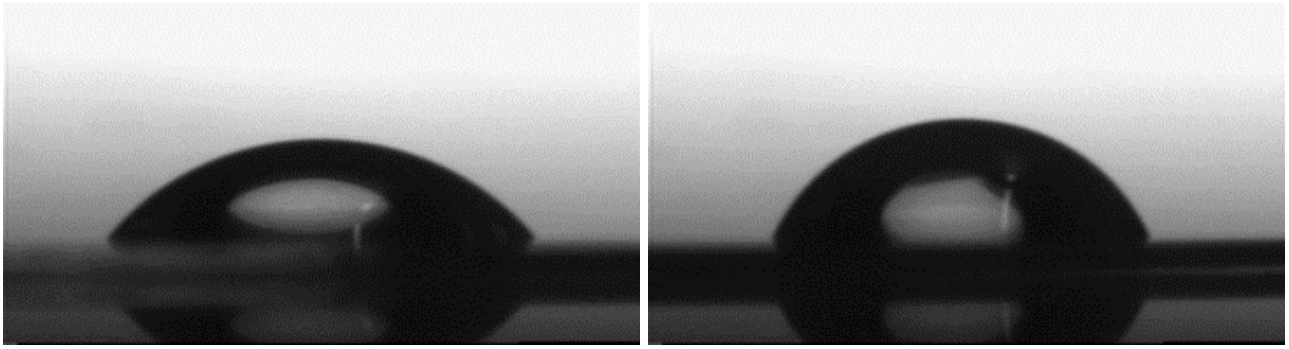

(a) (b)

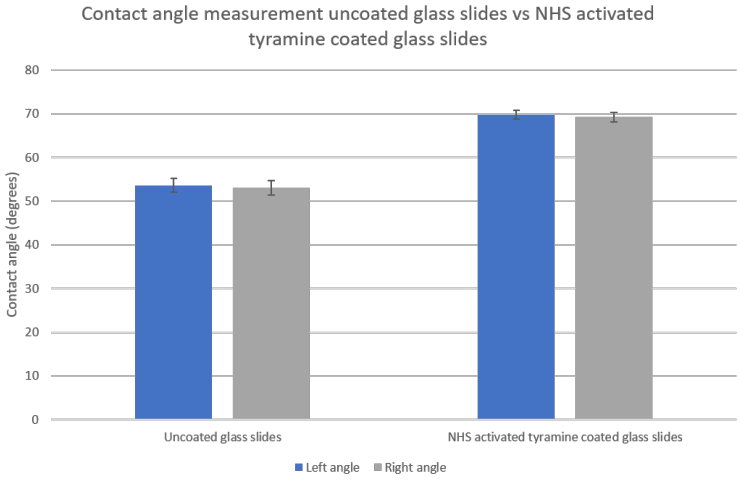

(c)

Figure 3.5: **Contact angle measurement**. (a) Representative picture of a water droplet on top of an uncoated glass slides, (b) Representative picture of a water droplet on top of a NHS activated tyramine coated glass slides, (c) Graph depicting the exact contact angles in degrees of the left and right side of the water droplets on top of the uncoated glass slides versus the NHS activated tyramine coated glass slides. This experiment has been performed with n=7.

can be mixed through.

GelTA(-MWCNT) does not attach to a TMS-PMA coating, so a new coating had to be found. It was decided to use a coating of NHS activated tyramine. The first step to achieve this is binding OH (hydroxyl) groups to the glass slide, which can be done with the Femto Science CUTE oxygen plasma cleaner. Afterwards the glass slides are submerged in (3-aminopropyl)triethoxysilane (APTES, 98%), obtained via Sigma-Aldrich, diluted in ultra pure water to a concentration of 3%. The glass slides are submerged for 30 minutes at room temperature. The incubation with APTES leads to the binding of primary amines to the glass slides. The unbound amines are then removed due to thorough washing of the glass slides with water. The next step is the binding of tyramine groups to the amines on the glass slides. This is achieved by submerging the glass slides in a NHS-tyramine (3-(4-hydroxypheyl) propionic acid N-hydroxysuccinimide ester (obtained via Sigma-Aldrich) solution for 10 minutes ate 4 °C. The solution was made by first slowly dissolving the NHS tyramine ester in DMSO after which it is diluted in bicarbonate reaction buffer at a pH of 8.4, to a concentration of 0.5 mg/mL. After thorough rinsing with water, the coated glass slides were then used within a day.

To verify whether the protocol works, a contact angle measurements has been done, of which the results are shown in Figure 3.5. In figure Figure 3.5 (a) and (b) pictures are shown of the water droplets on top of the (un)coated glass slides, while (c) shows the exact contact angles, with n=3. From Figure 3.5 it can be seen that the NHS activated tyramine coated glass slides are significantly more hydrophobe than the uncoated glass slides, showing that the coating protocol was effective.

It was however seen that whereas the center of the glass slide was very well coated with homogeneous angles being measured, towards the edge of the glass slide the coating was no longer homogeneous. This should be taken into account when making gel layers on top of the glass slides.

3.2.4 Cell attachment

As the influence of the hydrogel on the cultured CM is being researched here, it is important for the CM to be attached to the hydrogel in order to analyze the interaction between the hydrogel and the cultured CM.

It was first observed that the CM had trouble attaching to the GelMA gel layer. This can be seen in Figure 3.6, where the formation of cell aggregates indicates bad cell attachement, as a monolayer formation where the CM are in contact with the hydrogel would be ideal. The attachment of the CM to the GelMA as a percentage of the hydrogel layer has also been analyzed with the software ImageJ, where an attachement percentage of 24% was found.

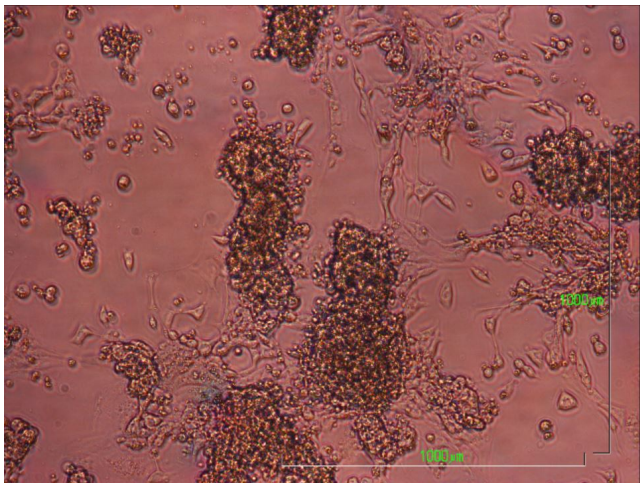

Figure 3.6: **Attachment of CM to GelMA**. To validate the attachment possibilities of CM to GelMA, the CM are cultured on top of GelMA hydrogel layers. A representative image from n=10 is shown.

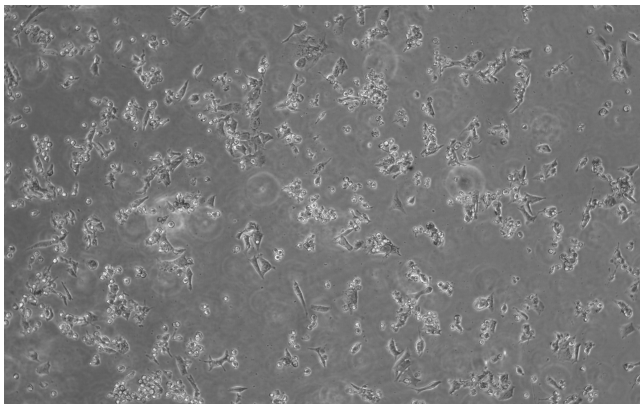

Figure 3.7: **Attachment of HepG2 cells to GelMA**. To validate the attachment possibilities of cells to GelMA, HepG2 cells are cultured on top of GelMA hydrogel layers. A representative image from n=4 is shown.

To validate whether other cell types can attach to GelMA, HepG2 have also been cultured on top of the GelMA, as can be seen in Figure 3.7. From this it can be seen that there is a possibility for cells to attach to GelMA.

To improve the attachment of the CM to GelMA, it has been researched whether the 10x TriplE used in the dissociation protocol, had a negative effect on the attachment of CM to GelMA. Another possibility for dissociating CM, is using 1x TriplE. Due to the lower TriplE concentration, it is possible that the attachment sites of the CM are disrupted less when using 1x TriplE, enabling the CM to form a better attachment to a new scaffold. The result of this comparison is shown in Figure 3.8. From this results, it is shown that the use of 1x TriplE gives a better attachment of the CM to the GelMA. The attachment of the CM to the GelMA as a percentage of the hydrogel layer has also been analyzed with the software ImageJ. An attachement percentage of 32% was found in the CM dissociated with 1x TriplE and 14% in CM dissociated with 10x TriplE.

The attachment of the CM to GelMA was still not ideal, as it can be seen that separate cell aggregates

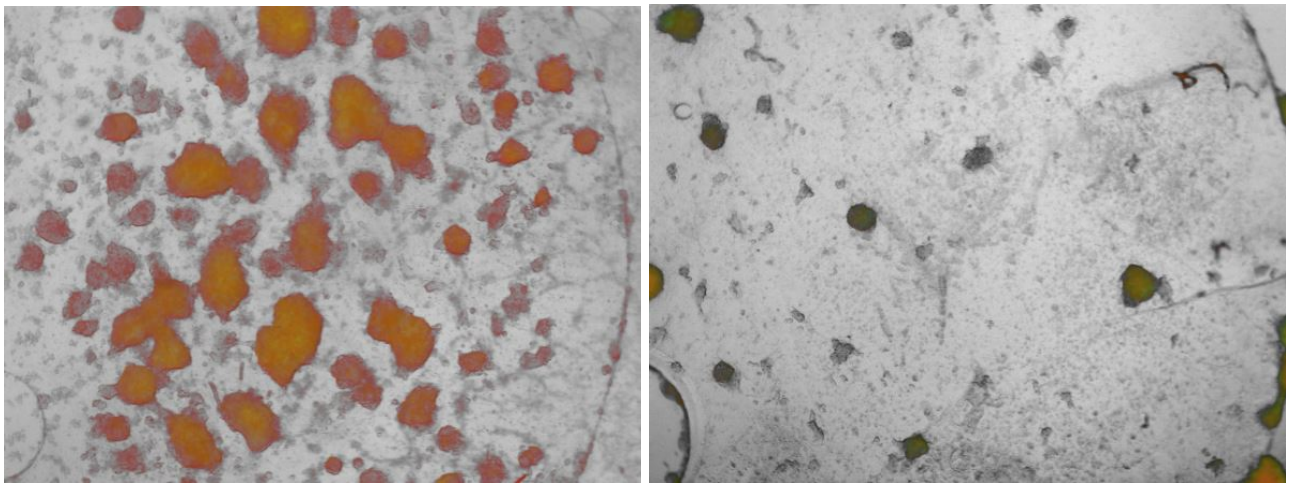

(a) (b)

Figure 3.8: **Attachment of CM to GelMA dependent on the TriplE concentration**. (a) Shows the attachment of CM cultured on top of GelMA when they are dissociated with 1x Triple. (b) Shows the attachment of CM cultured on top of GelMA when they are dissociated with 10x TriplE. Representative images from n=8 are shown.

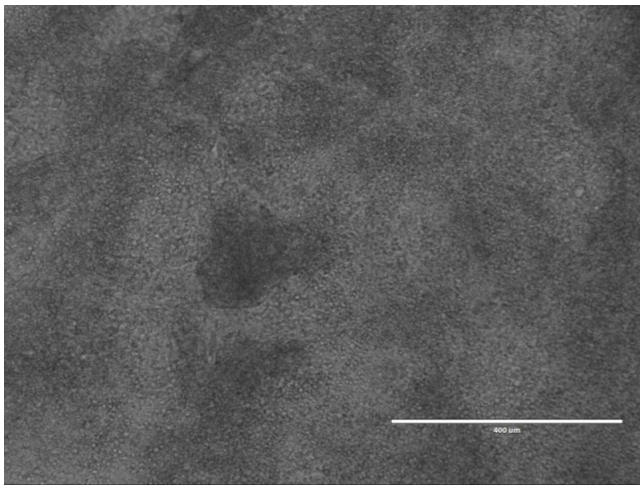

Figure 3.9: **Attachment of CM to GelTA**. To validate the attachment possibilities of CM to GelTA, the CM are cultured on top op the GelTA hydrogel layers. A representative image from n=6 is shown.

are formed instead of a desired monolayer with more cell-cell contact.

The CM cultured on GelTA show better attachment, as can be seen in Figure 3.9.

To verify to which GelTA percentage the CM attach best, the attachment of the CM to the GelTA as a percentage of the hydrogel layer has been analyzed with the software ImageJ for 10% GelTA, 8.5% GelTA, 7.5% GelTA, 6.5% GelTA, 5% GelTA and 3.5% GelTA after 11 days as this is the amount of days after which the maturation of the CM will be analyzed. Below 3.5% GelTA the hydrogel degenerated within 4 days and it was no longer possible to see the hydrogel layers and therefore it was not possible to analyze the percentage of CM attachment to the hydrogel layers. The attachment percentage is defined as the area of the hydrogel layer to which the CM are attached (this area can be obtained with the binary plugin from ImageJ) as a percentage of the total area of the hydrogel layer. As each hydrogel layer is fabricated with the same thickness and the same amount of GelTA solution, the total area of each hydrogel layer is similar. On each hydrogel layer the same amount of CM is seeded. Due to these similar conditions, the area of the hydrogel to which the CM are attached can be used as a measurement to determine to which GelTA percentage the CM attach best. Table 3.1 shows these attachment percentages with n=2. To make for a more reliable outcome, the experiment was repeated for 8.5% GelTA, 7.5% GelTA and 6.5%. Even though 10% GelTA also had a high attachment percentage, there were a lot of aggregates present in the wells, so this percentage was excluded. The results from the second experiment with n=3 are shown in Table 3.2. Due to these results, it has been chosen to culture the CM on 7.5% GelTA.

GelTA percentage	Percentage of CM attachment
10% GelTA)	46
8.5% GelTA	46
7.5% GelTA	46
6.5% GelTA	42
5% GelTA	41
3.5% GelTA	41

Table 3.1: **CM attachment.** The attachment of the CM to the different GelTA percentages is shown as the area of the hydrogel to which the CM have attached as a the percentage of the area of the total hydrogel layer. The average of n=2 is shown.

GelTA percentage	Percentage of CM attachment
8.5% GelTA	60
7.5% GelTA	70
6.5% GelTA	42

Table 3.2: **CM attachment repeated experiment.** The attachment of the CM to the different GelTA percentages is shown as the area of the hydrogel to which the CM have attached as a the percentage of the area of the total hydrogel layer. This table shows the repeat of certain percentages. The average of n=3 is shown.

3.2.5 Reproducibility of fabricating thin hydrogel layers

As could be seen from Figure 3.2, the spacers used to fabricate the thin GelMA layers in the initial fabrication protocol, are 3 layers of scotch tape taped on top of each other. As the tape cannot be properly cleaned, the spacers have to be remade for the fabrication of every single hydrogel layer, making this method labor intensive . It is also not reproducible due to errors in the placing of the tape layers, leading to differences in the spacers.

Therefore I have worked on creating a more facile and more reproducible method for the creation of the thin hydrogel layers. For this I decided to make a mold from PDMS, to which the GelMA should not attach. I made this mold by placing a small piece of PMMA in a wells plate and pouring PDMS on top. After curing the PDMS, the PDMS is taken out of the wells plate and the PMMA be removed, leaving a PDMS mold. By placing a drop of GelMA within the PDMS mold and placing a TMS-PMA coated glass slide on top of this drop, the hydrogel layer should attach to the glass slide after UV curing. This idea is visualized in Figure 3.10 (a). The manufactured molds are shown in Figure 3.10. After several tests with GelMA in the PDMS mold, it was decided that the mold does function, as the GelMA attaches to the coated glass slide placed on top. The mold was still not optimal though, due to the fabrication process of the mold not being reproducible as the PMMA moves around in the PDMS. Therefore I decided to make an inverse of the PDMS mold in Solidworks, to mill into PMMA. On this PMMA mold PDMS can then be poured to easily produce more PDMS molds. The PMMA milled mold is shown in Figure 3.10 (c). This made for a facile, reproducible fabrication method of thin GelMA layer.

It was found that the GelTA(-MWCNT) attached to the PDMS mold as well as the glass slides. Therefore it was not possible to use the PDMS mold for the fabrication of the thin hydrogel layers. While performing the measurements to obtain the viscoelastic properties of the GelTA(-MWCNT), see subsection 4.1.1, it was asses that the GelTA(-MWCNT) does not attach to PMMA. This means that it would be possible to make a PMMA mold, similar to the PDMS mold, for the fabrication of the thin GelTA(-MWCNT) hydrogel layers. Unfortunately I was not able to try this because the milling machine was out of service for a long time during my master thesis. When continuing this project, designing a PMMA mold might make for a more facile production method of the thin hydrogel layers.

Instead, the method I used for the production of the thin hydrogel layers is similar to the initial concept for the fabrication of the thin GelMA layers, as can be seen in Figure 3.2. The difference is that in stead of using UV light for crosslinking, I use 0.3% H_2O_2 to activate the HRP in the GelTA(-MWCNT), causing the GelTA(-MWCNT) to form a gel. The time between adding the H_2O_2 and the crosslinking of the GelTA(-MWCNT) is dependent on the percentage of HRP in the GelTA(-MWCNT). The fabrication of the thin GelTA(-MWCNT) layers is therefore as follows, as can be seen in Figure 3.11. Instead of placing the coated glass slide on top of the gel, I attached the coated glass slide in between 2 spacers. As I did not find sticking multiple layers of scotch tape on top of each other a facile method nor entirely reproducable (as it is hard to stick the multiple layers exactly on top of each other), I used a tape with a thickness of 50 μm so I only had to use 1 layer. I then deposited a drop of 8 μL GelTA(-MWCNT) on top of the coated glass slide, after which I pipetted 6.25% 0.3% H_2O_2 through the GelTA(-MWCNT)

drop. Immediately, so as to act before the GelTA(-MWCNT) started to harden, I placed an uncoated glass slide on top of the drop to flatten it and create a thin GelTA(-MWNCT) a layer.

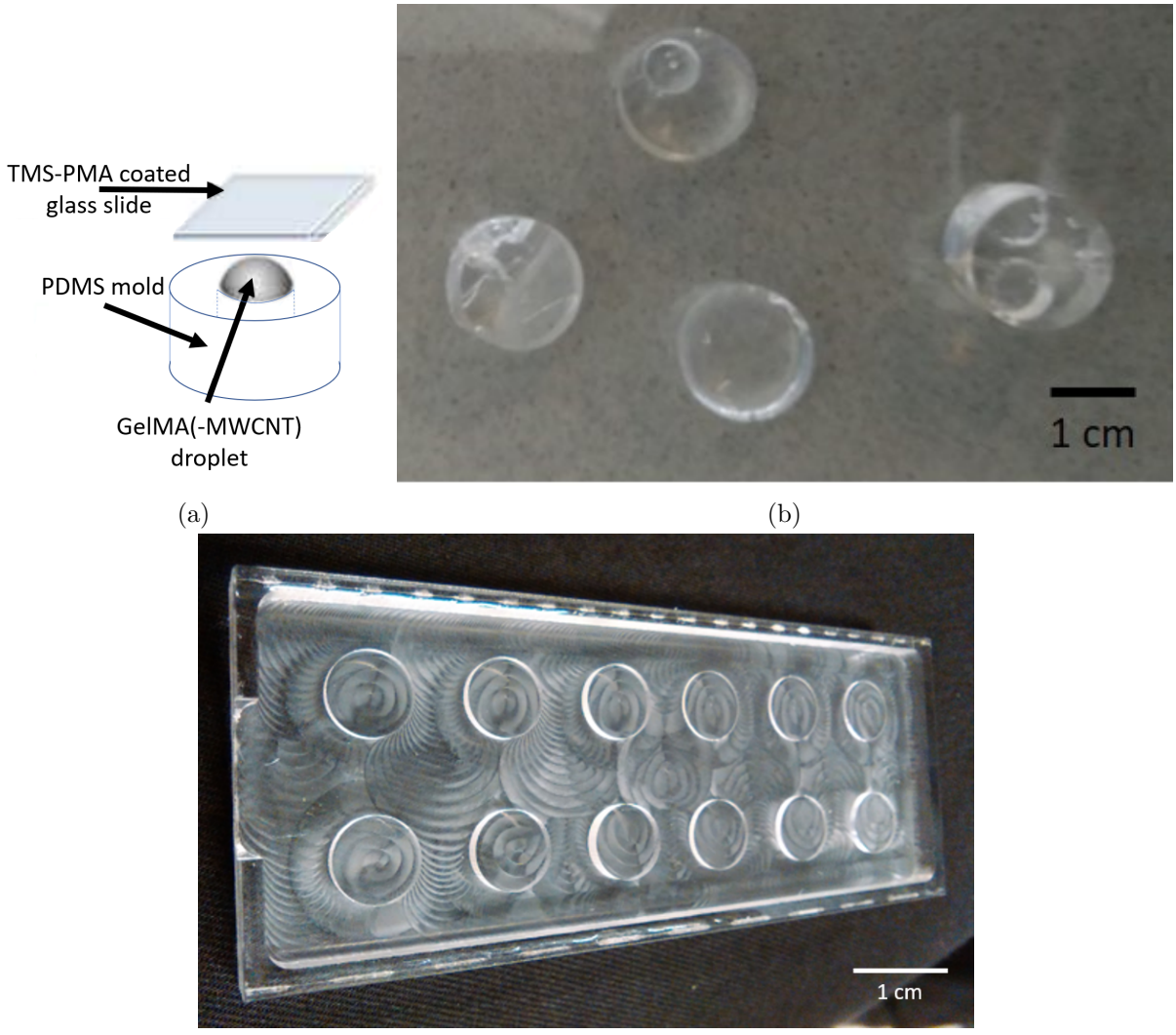

(a) (b)

(c)

Figure 3.10: **Fabrication of thin GelMA(-MWCNT) layers**. (a) A polymer drop is placed within a PDMS mold, after which the drop is flattened with a coated glass slide. UV curing causes the polymer to crosslink, not visualized in this figure. (b) PMMA inverse of the PDMS mold, to be able to pour PDMS mold. This experiment has been performed with n=5. The figure shows various stages of success, with the left and bottom mold not showing an indent to place the GelMA(-MWCNT) droplet in the PDMS. Both the top and right mold show this indent, but the placing in the GelMA is random, not making for a reproducible method. (c) shows the PMMA milled mold for the reproducible fabrication of GelMA hydrogel layers.

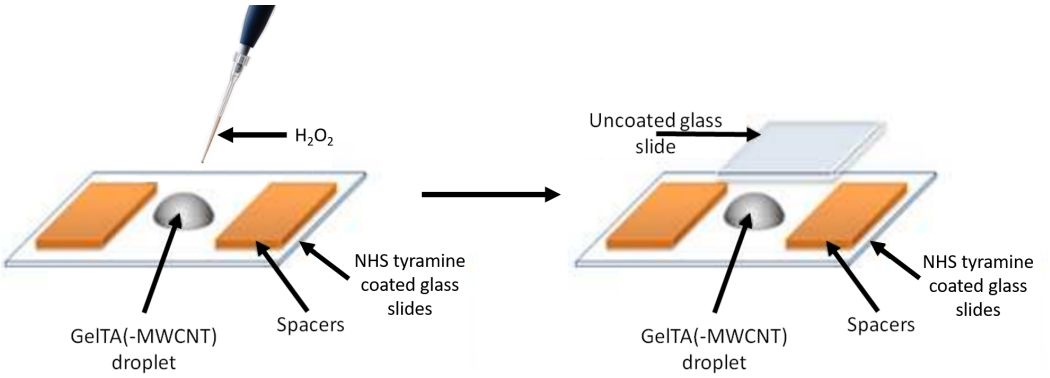

Figure 3.11: **GelTA hydrogel layer fabrication.**

3.2.6 3D cardiac model

As 3D cardiac models are more representative of the *in vivo* heart than monolayers, creating a 3D cardiac model is an improvement of the initial concept, where 2D cardiac monolayers were cultured. As GelMA-MWCNT did not cure throughout the entire thin hydrogel layer, it was not managed to make a thicker 3D cardiac model with GelMA-MWCNT. Therefore GelTA-MWCNT has been used to improve the inital concept by making a 3D cardiac model.

Instead of seeding CM on top of thin hydrogel layers as is done in the initial concept, 1.8 million CM are gently resuspended in the desired amount of GelTA(-MWCNT), for which 100 μL was used. The GelTA(-MWCNT) including the CM is pipetted in a drop on top of the coated glass slides. To crosslink the GelTA(-MWCNT) 11.2 μL H_2O_2 is then gently mixed through the drop, causing the GelTA(-MWCNT) to harden and a 3D model to be formed.

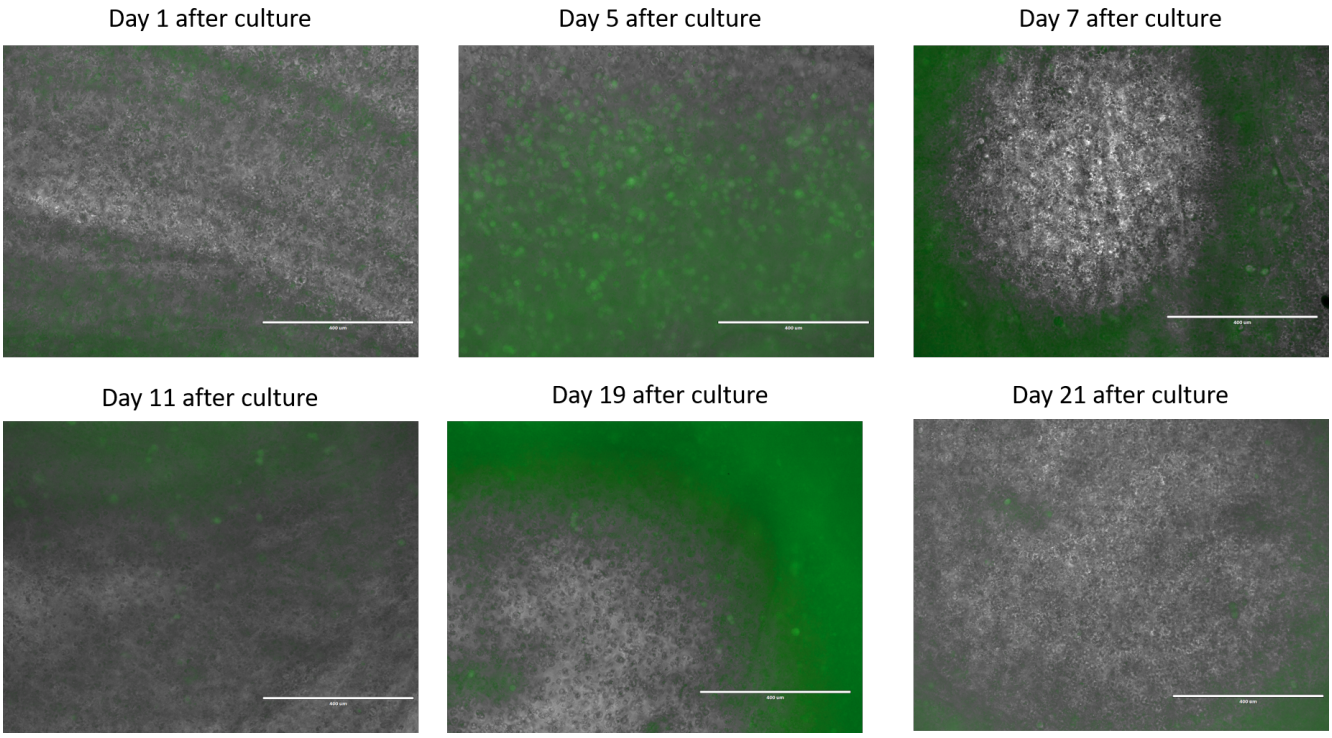

Figure 3.12: **CM cultured in GelTA**, the CM are monitored at multiple time points. No migration is seen over time.

To validate the 3D cardiac model, the migration of the CM over time has been monitored. CM migration is necessary for the CM to make cell-cell contact, which is necessary to create a 3D cardiac model which mimics the *in vivo* cardiac tissue.

No visible migration of CM was observed when using this method, as shown in Figure 3.12, just as there were no visible contractions. This meant that the protocol used for creating 3D cardiac models had to be adapted to create a functional 3D cardiac model, for which multipe steps have been taken.

GelTA percentage

As just shown, 'simply' mixing cells through a drop of GelTA(-MWCNT) did not result in a functional 3D cardiac model. To create a functional 3D cardiac model is has been looked into whether using multiple percentages of GelTA affects the migratory abilities of the CM. The experiment was done by suspending 1 million CM in 50 μL of 5% and 10% GelTA. Figure 3.13 shows no visible migration over time, independent on the GelTA percentage. Multiple time points have been monitored, but for visibility only the first and last time point are shown.

Cell density

It has also been investigated whether the cell density could affect the migration of the CM through the GelTA and thereby the functionality of the 3D cardiac model. This was based on the idea that it was possible that the reason behind the static behavior of the CM was caused by the CM not sensing the surrounding CM. Therefore the CM are not aware that they can connect to other cells and therefore will not migrate towards these other cells. An idea to overcome this, was to increase the density of cells seeded in the GelTA. When there are more CM in the scaffold, the CM are closer together and might be more aware of the surrounding CM which could stimulate the migration of the CM. To validate this theory, different cell densities have been seeded, being 1.5 million CM in 100 μL GelTA, 2 million CM in 100 μL GelTA, 2.5 million CM in 100 μL GelTA and 3 million CM in 80 μL GelTA, which is similar to 3.5 million CM in 100 μL GelTA. The cultures have been monitor over time, the results of which can be seen in Figure 3.14. The 3D cultures were visualized after 4, 6, 8, 11 and 13 days. As can be seen, no

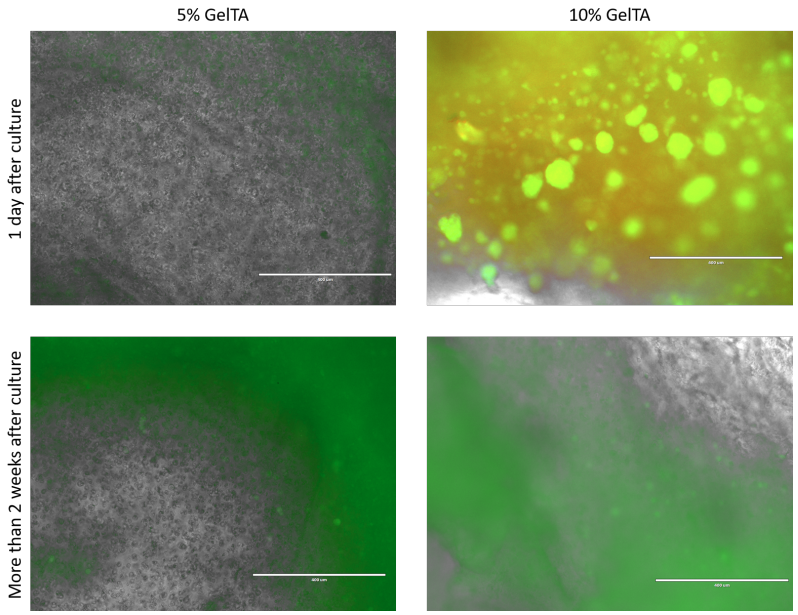

Figure 3.13: **CM in 5 % and 10 % GelTA percentages over time.** CM cultured in 5 and 10 % GelTA monitored over multiple time points. No visible migration is shown at any time point.

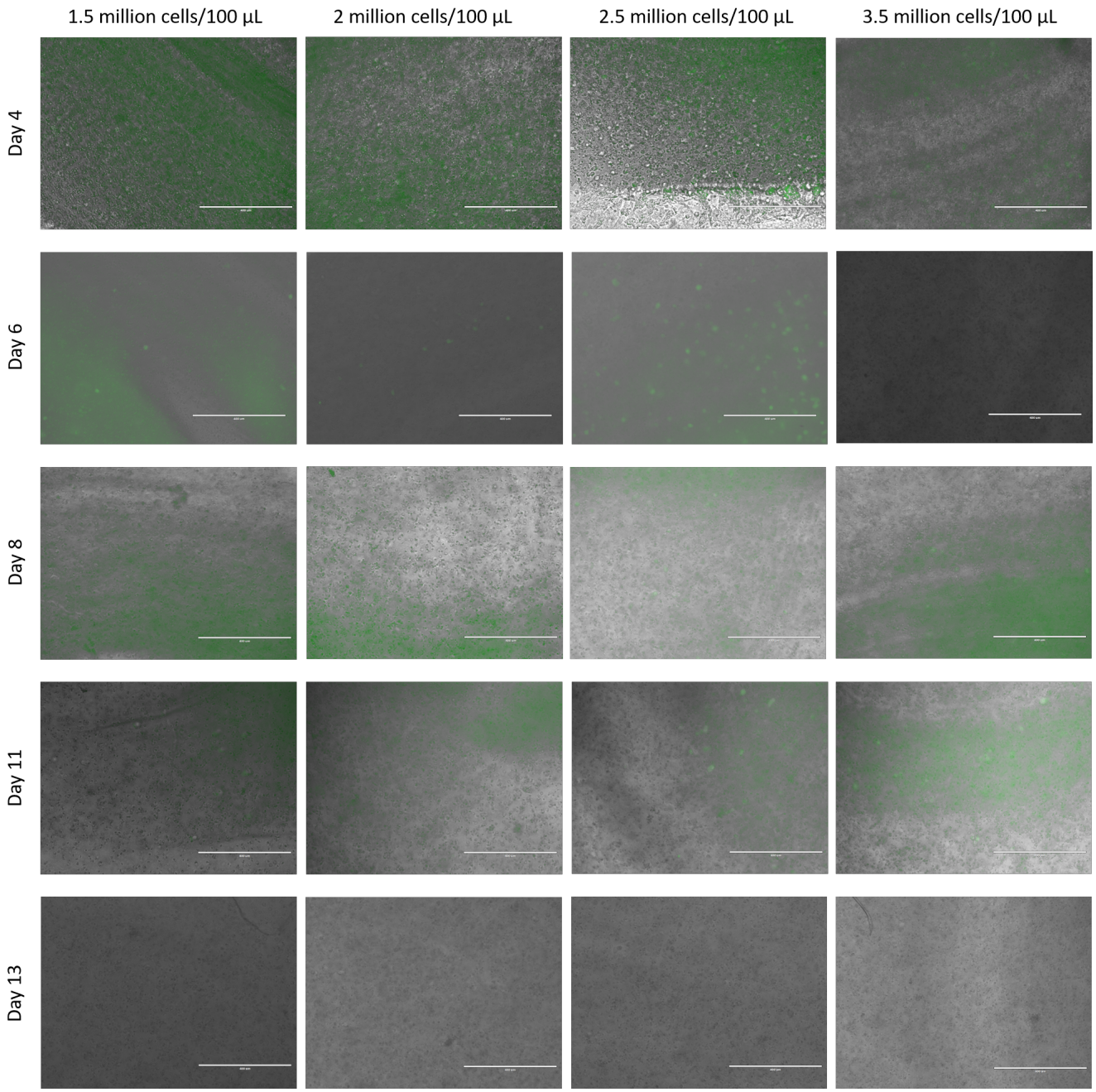

Figure 3.14: **Cell densities over time.** Different cell densities cultured in GelTA monitored over multiple time points. No visible migration is shown at any time point.

migration was visible in any of the conditions after any of the time points. The theory could thus not be validated.

Poly(ethylene) oxide

As discussed in subsection 2.1.4, using the aqueous two-phase system of GelTA and PEO should theoretically create an interconnected pore network, tunable in size, in the GelTA 3D model. This should stimulate the migration of the CM through the GelTA, creating a better 3D cardiac model. For the experiment done to validate this method 1.6% PEO in DPBS was mixed 1:1 with 10% GelTA, resulting

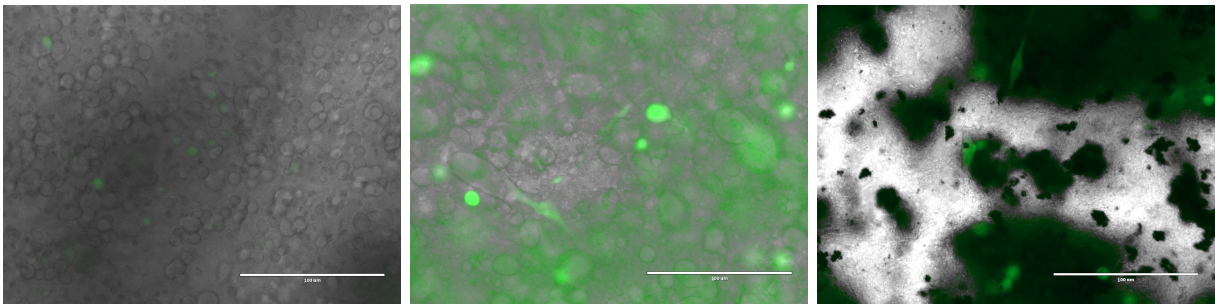

(a) (b) (c)

Figure 3.15: **CM in GelTA(:PEO(-MWCNT))**. (a) CM cultured in pristine 5% GelTA. (b) CM cultured in 5% GelTA:PEO. (c) CM cultured in 5%GelTA:PEO-MWCNT. Samples are analyzed with n=2 and a representative image is shown here. The CM are shown in green, with the round CM showing no migration and the stretched CM showing migration. The scale bar in each figure represents 100 μm.

in an end percentage of 5% GelTA.

CM have been cultured within pristine 5% GelTA, 5%GelTA:PEO and 5%GelTA:PEO with 1 mg/mL MWCNTs with n=2. The results of this are shown in Figure 3.15. Figure 3.15 (a) shows the (absence of) migration of CM through pristine 5% GelTA after 14 days. Figure 3.15 (b) shows the migration of CM through 5%GelTA:PEO after 14 days. Figure 3.15 (c) shows the migration of CM through 5%GelTA:PEO with 1 mg/mL MWCNTs after 14 days.

From these figures it can be seen that in pristine 5% GelTA the CM have not been migrated, whereas they have migrated in both 5%GelTA:PEO and 5%GelTA:PEO with 1 mg/mL MWCNTs. Though a migration is visible, it is not enough to create a network where all CM have cell-cell contact. To make for a scaffold with better CM migration, the ratio of GelTA:PEO can be adapted. The PEO percentage can also be altered. It is also possible to increase the molecular weight of the PEO, as this can increase the phase separation between GelTA and PEO, making for a possible 3D cardiac model via the aqueous two-phase system of GelTA and PEO. [7]

3.3 Optimized protocol

In this section, the optimized protocol developed in this master thesis to create homogenously thin hydrogel layers of GelTA(-MWCNT), will be discussed step by step, starting after the production of GelTA.

Glass coating

For the GelTA to attach to the glass slides, the glass slides first need to be coated with NHS activated tyramine.

- Dissolve NHS activated tyramine in a small amount of DMSO, till everything is dissolved.
- Add CB buffer, with a pH of 8.4, to the solution, with steps of 100 μL CB buffer, till a final concentration of 0,5 mg/mL NHS activated tyramine.
- Treat the glass slides with the oxygen plasma treater set on the 2nd program.
- Spread 30 μL 3% APTES out over each glass slide.
- Incubate at RT for 30 min.
- Aspirate the APTES.
- Rinse the glass slides twice with ethanol.
- Rinse a final time with distilled water.
- Dry the glass slides as much as possible with the N_2 tap.
- Spread 30 μL NHS activated tyramine out over each glass slide.
- Incubate at 4 °C for 10 min.

- Aspirate the APTES.
- Rinse the glass slides twice with ethanol.
- Rinse a final time with distilled water.
- Dry the glass slides as much as possible with the N_2 tap.
- Store at 4 °C and use within a day.
- Be sure to mark or remember which side of the glass slides is coated.

Making the necessary solutions

- First, dissolve GelTA in DPBS, creating a solution of 13.6% GelTA. Dissolve the GelTA in a warm water bath, at around 37 degress Celsius.
- While the GelTA is dissolving, dissolve HRP in DPBS, resulting in a concentration of 40 units/mL.
- Make a concentration of 0.3% H_2O_2 in DPBS.
- In an eppendorf tube, add 80 mg MWCNT and 300 mg GelTA.
- Dissolve in 4 mL DPBS, this is the MWCNT stock solution.
- Sonicate the MWCNT stock solution for 30 minutes with the Branson Ulrasonic Sonicator S-250A probe sonicator with a duty cycle of 60% and an output of 4.
- After the GelTA has completely dissolved, add Horse Radish Peroxidase (HRP) at a 10:80 HRP:GelTA ratio.
- Make the solutions with the desired different amounts of MWCNT according to Table 3.3, in 1.5 mL eppendorf tubes. By following the ratios from Table 3.3 each condition has a GelTA percentage of 7.5. For each thin hydrogel layer, 8 μL solution is required, so multiply the amounts from Table 3.3 according to the amount of hydrogel layers to be made. Of course different concentrations of MWCNT can also be mixed through the GelTA in the same fashion.
- To make a solution with an amount of MWCNT higher than 9 mg/mL, a stock solution with a higher concentration of MWCNTs has to be made.
- Be sure to thoroughly mix the MWCNT through the solutions, to create a homogeneous solution.

End amount of MWCNT in the solution in mg/mL	Amount of 13.6% GelTA in mL	Amount of GelTA coated MWCNT stock in mL	Amount of DPBS in mL
0 (pristine 7.5% GelTA)	33	0	27
1	33	3	21
3	33	9	15
5	33	15	9
7	33	21	3
9	33	27	0

Table 3.3: **GelTA:MWCNT ratio's.** In this table the ratio's of 13,6% GelTA:GelTA coated MWCNT stock solution used to fabricate each separate gel condition are shown.

Fabricating the thin hydrogel layers

- Store the 1.5 mL eppendorf tubes with the solutions in a 1 mL tube box filled with water, at around 40 °C to keep the solutions liquid.
- Store the H_2O_2 on ice.
- Put the coated glass slides on a petridish and cover them with tape with a thickness of 20 μm, leaving a 1 cm gap between them, as can be seen in Figure 3.11.
- Pipet 8 μL GelTA(-MWCNT) on the coated glass slide.
- Mix 0.5 μL H_2O_2 through the drop.
- Immediately place an uncoated glass slide on top of the drop to create a homogeneous thick layer.
- Wait 10 minutes before removing the top slide.
- Remove the spacers and place the coated glass slide with the hydrogel layer on top in a culture wells-plate.

- Store the finished hydrogel layers in the incubator for a day before CM dissociation, make sure NOT to put any liquids on top of the hydrogel layers, as the surface tension of any liquids on top of the hydrogel layers will cause the CM to flush off the layers during dissociation, before the CM have time to attach to the hydrogel.

CM dissociation

- Aspirate medium from the wells.
- Wash cells with 1 mL PBS, aspirate.
- Add 1 mL 1x TryplE
- Place plate in an incubator for 15 min.
- Tap plate to detach cells.
- Place plate back in an incubator for 15 min.
- Tap plate to detach cells.
- Most CM should be detached now, but carefully dissociate the rest by pipetting up and down with a p1000 biosphere pipette tip.
- When too many clumps remain, place plate back in the incubator for a few minutes and pipette up and down again.
- Add 4 ml of the medium in which the cells will be dissociated in a 15 ml tube and add the cells to inactivate the 1x TryplE.
- Spin down at 240*g for 3 min.
- Aspirate and resuspend in 2 mL of the medium in which the cells will be dissociated.
- Filter with filter FACS tube, wash old tube with 0.5 mL of the medium in which the cells will be dissociated, add to FACS tube.
- Count the cells using a counting chamber.
- Adjust the amount of medium in the tube to make a concentration of 500k cells/70 μL.
- Plate down the 500k cells/70 μL on the hydrogel layers in the culture wells-plates.
- FACS a remainder of the cells to determine the percentage of cardiomyocytes.
- Be sure to refresh the medium the day after dissociation.

Chapter 4

Experimental Methods

The experiments will be discussed in the following order: first, the gel characterization will be discussed, which consists of viscoelastic measurements and conductivity measurements. Then, the experiments performed to determine the maturation of the cardiomyocytes are explained.

Each experiment will start with a small theoretical introduction, leading to the methods. The results and discussion are shown chapter 5.

4.1 Gel Characterization

4.1.1 Viscoelastic properties

Theory

With rheology experiments viscoelastic properties of materials are measured, including the G' and G". Here G' is the elastic modulus also called the storage modulus, storage of elastic energy. G" is the viscous modulus, which describes the viscous dissipation. Thus, G" describes the behavior of the material while it is being deformed, whereas G' describes the behavior of a material after it has been deformed.

The G' is the relation between the force per applied area (stress) and the fractional stretching (strain), which is the same as Young's modulus, and the G" is the relation between the change in strain over time which happens after the removal of the applied stress. [44] [45] [46]

These material characteristics are measured by putting the material between two plates, one of which is rotating. The rotation causes deformations within the material, which are then measured. [47]

For cardiac tissue, the physiological Young's modulus is 5-10 kPa and >50 kPa for scar tissue at an infarct. [48]

Methods

- Determine the ratio of HRP:GelTA(-MWCNT) so the gelification process takes at least 30 seconds, giving you enough time to pipet the hydrogel in the mold before it solidifies. For the experiments performed in this master thesis, this ratio is 3.333:80.
- Take the mold used for fabricating gels for the rheology experiment and clamp an (uncoated) microscope slide on top of the mold, shown in Figure 4.1
- Mix a ratio of 5:80 H_2O_2:GelTA(-MWCNT) through the GelTA(-MWCNT)-HRP and immediately pipet 400 μL into the mold.
- Let the blend gelify for 10 minutes.
- When making multiple gels, thoroughly clean the mold between conditions.
- Make the gels a day before the rheology measurement and store them in DPBS.

- With a spatula, remove one of the gels from the glass slide and push it under the plate.
- Set the measurement height to 1.9 cm to be able to push the gel to be perfectly aligned with the probe.
- Set the measurement height so the measured force is 0.5 N.
- Set the temperature at 20 °C.
- Measure the frequency at which a stable storage modulus is measured with a frequency sweep.
- Measure the strain at which a stable storage modulus is measured with a strain sweep.
- Set these values and don't change them between conditions.
- Set the amount of measuring points to 18, each taking 5 secs, so the total measurement takes 90 sec per condition.
- Set the measurement height to 10 cm.
- Perform the measurement, an equilibrium should be achieved within 3 data points.

4.1.2 Conductivity

Theory

In order to determine the effect of conductivity of the scaffold on the maturity of cardiomyocytes, the conductivity of the scaffolds has to determined. A four point probe measurement, also called IV measurement, is a way to achieve this. The four point probe designed for this master thesis is shown in Figure 5.2 (a). It is important that the spacing between the probes is equal. As the name suggests, four probes are placed in the hydrogel, shown in Figure 5.2 (b). These probes can be different materials, but due to the previously mentioned high conductance and inert nature, gold will be used for this master thesis. An isolating layer is placed at the top of the probes, to ensure all current passed through the probes enters through the gel and not through the connection between the probes. The probes are connected to the HF2IS Impedance Spectroscope with cables. A current I is passed through the two outer probes, which causes a potential difference over the gel. This can be measured as a voltage V over the inner

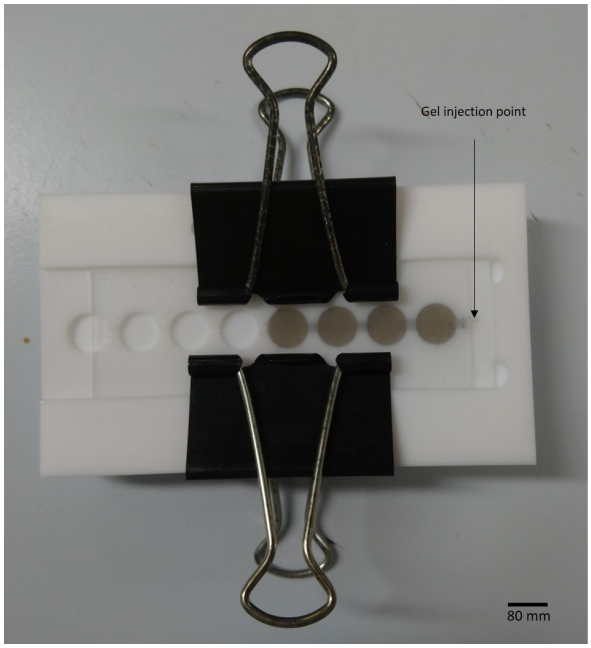

Figure 4.1: **Mold rheology gels**. The mold used for the fabrication of hydrogels for the performance of a rheology measurement, at the left side there is an opening for the injection of the hydrogel.

two probes. A similar measurement could be done with a two point probe, but the gel can interact with the probes, creating a resistive oxide layer, an electrical double layer, around the probes. With only two probes present, this electric double layer plays a major role in the measured resistivity. However, with four probes present and the voltage being measured over the inner two probes, where no current is applied, the electrical double layers will only form around the outer two probes and not influence the measured voltage. Therefore, with a four point probe it is possible to obtain a material property, whereas with a two point probe the measured conductivity is also experiment dependent and therefore not strictly a material property. The geometry of the measured samples is less important in a four point probe than in a two point probe, but when different samples will be compared measures should still be taken to make the geometries as equal as possible to prevent the geometry from influencing the outcomes.

From the performed measurements, the material resistivity can be calculated with Equation 4.1:

$$\rho = 2\pi s \frac{V}{I} \tag{4.1}$$

With ρ the material resistivity, s the spacing between the probes, V the measured voltage across the inner probes and I the applied current through the outer probes. [49]

Methods

The methods for performing a four point probe measurement are pretty self explanatory from the before described theory.

The gels with the desired conditions need to be made beforehand in similar boxes, to ensure similar geometries. It is important to fill the boxes enough so that the conducting gold parts of the probes can enter the gel completely. The probes should be slowly descended into the gel, making sure not to move them in x or y axis so as not to disrupt the gel.

The measurements are done at frequencies ranging from 100 Hz to 1 kHz.

After the measurement have been performed, the probes were slowly pulled from the gel, making sure not to move them in x or y axis so as not to disrupt the gel. To probes were cleaned with a tissue so as to ensure that possible gel remnants were removed after each measurement.

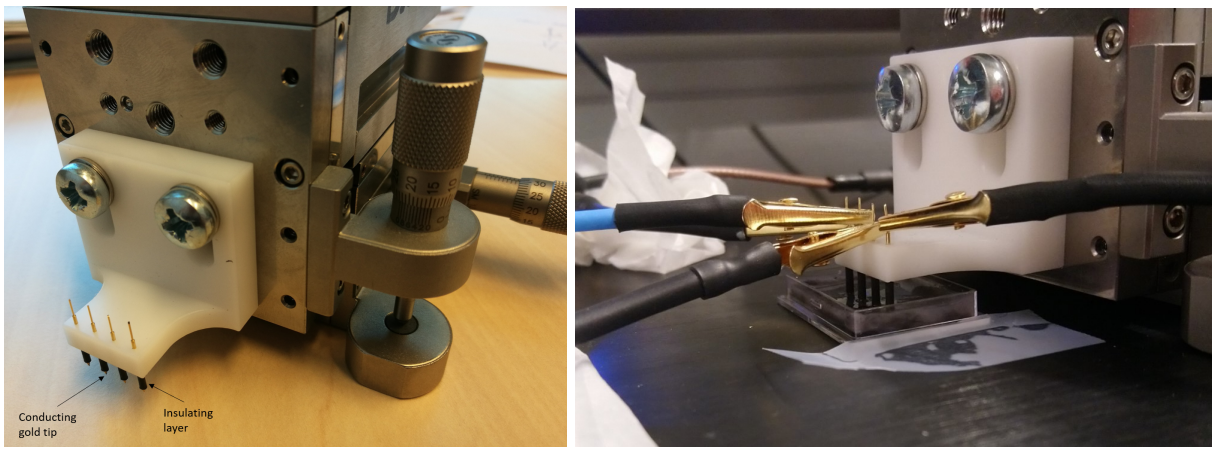

(a) (b)

Figure 4.2: **Four point probe set-up**. (a) The four point probe device, made specifically for this master thesis. The probes are attached to a holder which can be controlled in the x- y- and z-axis. The probes are spaced equally apart with a distance of 1 cm between them. The handle to use for this control is shown on the right. Also, the conducting gold tip and insulating layer around the gold tip are indicated. (b) The probes are connected to a Impedance Spectroscope via cables and positioned in the hydrogel.

4.2 Cell characteristics

For the assessment of general cell characteristics the viability and contractility of the CM will first be explained.

The main question of this master thesis is to evaluate whether there is a difference in maturity between CM cultured on GelTA and CM cultured on GelTA-MWCNT. To be able to answer this question, characteristics associated with maturity have been discussed in section 2.4. How to measurure these characteristics will be explained here. CM cultured on GelMA-SWCNT showed more maturity characteristics than CM cultured on pristine GelMA after 8 days in culture. [21] The CM cultured during this master thesis are therefore also expected to be able to show differences in maturity already after 8 days. To give the CM a few more days to display more maturity characteristics, the CM will be investigated after 11 days in culture. To make for reliable results, 3 different dissociation runs will be performed, each with at least n=4, to have enough samples for a reliable analyses.

4.2.1 Viability staining

Theory

Though not a measure of maturity, the viability is still vitally important to asses the biological functionality of scaffolds. If the CM are not able to survive on a scaffold the scaffold cannot be used for tissue engineering. Simply put, the viability is the percentage of living (viable) cells of the total amount of cells. To differentiate between the types, all cells are stained. Cells are stained by adding a fluorescent dye. This dye can be cell permeable, actively or passively, which are generally molecules with a positive or neutral charge. The dye can also be cell impermeable, usually molecules with a negative charge, or bind to the cell membrane. The dye can become fluorescent by attaching to their binding site, or be fluorescent from the start. [50]

For a live-dead assay, the nuclei of the CM are stained with Hoechst, which is a positively charged molecule which is cell permeable and attaches to the minor groove of a DNA double helix, only present in the nucleus. As Hoechst is cell permeable, whereas DAPI is not, Hoechst is used for nucleus staining of living cells. DAPI is often used for nucleus staining of fixed and permeable cells as it is more stable than Hoechst. Hoechst has an excitation of around a wavelength of 350 nm and an emission at a wavelength of 461 nm, therefore it stains the nuclei blue. Simultaneously, the CM are stained with Ethidium homodimer (EtdH), which is a highly specific nucleic acid staining. EtdH is membrane impermeable. As nucleic acid is only located within the nucleus, EtdH will only be able to enter to apoptotic or necrotic cells which membranes are ruptured, allowing the EtdH to enter the cell and the nucleus and bind to the nucleic acid. EtdH has an excitation at a wavelength of 528 nm and an emission at a wavelength of 617 nm and therefore stains the nucleic acid red. When analyzing an EtdH staining, it should be taken into account that when cells and nuclei have ruptured it is possible that the contents have slipped out of the cell, therefore creating a background signal of EtdH. It is also possible to stain living cells green with Calcein. However, as the used CM are GFP positive, their will be too much background signal to be able to distinguish the stained nuclei from the GFP signal, such that Calcein cannot be used for this master thesis.

Methods

As the CM still let go of the scaffold relatively easy, the protocol has been adapted to forego some washing steps so as to prevent the CM from detaching and being washed away.

- First perform a quick washing step of the wells with DPBS.
- For the second washing step, leave the DPBS on for 5 minutes before aspirating.

- During these 5 minutes, make the staining solution, make sure not to expose the staining to light: For a 24 wells plate, 200 μL staining solution is required, but always be sure to make for 1-2 wells extra to be safe. Per 1 mL DPBS, add 1 μL EtdH and 1 μL Hoechst.
- After aspirating the DPBS, pipet 200 μL of the staining solution in each well and incubate for 30 minutes
- Aspirate the medium and perform another quick washing step with DPBS.
- For the second washing step, leave the DPBS on for 5 minutes before aspirating.
- Add 1 mL DPBS to each well. The plate can then be stored at 4 °C up to a few weeks.
- Images of separate channels the stained wells have to be taken in order to analyze the viability. A magnification of 40x is recommended for most accuracy regarding single cells.
- The program CellProfiler 3.1.8 can identify the amount of objects present in each channel. This has to be done by loading pictures of both channels per condition into the program. Both channels need to be identified as primary object and the settings, most importantly the minimal and maximal pixel size to identify the objects to be counted, have to be set on to be most reliable for the outcome. The most reliable being that only single cells are counted as such, so clumps of cells, background noise and artifacts are not identified as primary objects. For the Hoechst stained nuclei of all CM of the CM cultured in this experiment, these were decided to be between 25 and 85 pixels, as the nuclei had a rather large spread in size. For the EtdH stained nuclei, the dead cells, these were set to be between 25 and 60, due to a lot of blurry background noise which had to be excluded. For reliability it is important to keep these settings the same for each condition. For more reliability n=2 has been used.
- Finally, by dividing the number of identified dead cells n_{dead} by the identified total number of cells n_{tot}, a death ratio is obtained. The actual viability can be computed from this with $n_{life} = 1 - n_{dead}/n_{tot}$.

4.2.2 Contractility

Theory

As discussed in section 2.3, CM contract. The contractions of cultured CM can be monitored under a microscope. The spontaneous, meaning unpaced, contraction characteristics of the cultured CM will be analyzed here. These characteristics entail the contractility rate and maximum contraction and relaxation velocity. It is also possible to perform a patch-clamp recording of single cells to measure the membrane potential, which is higher in fetal CM than in mature CM. [51] [52]

Methods

Videos have been taken at 10x magnification of the spontaneous contractions of the cultured CM. The MotionGui software is used to analyze videos.

- 1/3 of the frames of the videos are saved and loaded into the MotionGui interface.
- The frame rate is left at a default of 14.
- The pixel size has been measured to be 0.71 μm.
- The motion vectors of the video can now be made.
- After the vectors have been obtained, click on the make a video button.
- After a video has been made, find the center of beating of the cardiomyocytes to be able to distinguish the movement between contraction and relaxation.
- Finally the contraction data can be obtained, analyzed and evaluated.

A detailed description on how to use the MotionGui software is available in [53].

For the assessment of maturity characteristics qPCR and immunostaining will be explained.

4.2.3 RNA expression of gene encoding for Cx43 protein from qPCR

Theory

tessa There are different types of Polymerase Chain Reactions (PCR) one of which is quantitative PCR (qPCR), used to quantify the amount of RNA molecules within a sample, relative to the samples analyzed, whereas PCR is used to analyze, or amplify, the presence of DNA. [54] By analyzing whether certain gene strands are present and in which ratio, information is gathered on the ability of a sample to express certain proteins. It should be taken into account that qPCR alone does not give information on the expression of the proteins, only the available opportunity for a sample, or cell, to facilitate this expression.

RNA has to be transcribed to cDNA, a process which is called reverse transcriptase, after lysating a tissue sample to gather RNA and isolating said RNA, as RNA is easily degradable. After the RNA is isolated, cDNA has to be formed. To allow for as little as possible inter-sample technical differences, the amount of RNA set to be transcribed into cDNA should be equal among all samples. For this, the amount of RNA in ng/mL is measured with a nanodrop. First the RNA is denatured, after which a primer binds to the RNA strand, reverse transcriptase binds deoxyribose nucleoside triohosphates (dNTPs), the building blocks of DNA a process called annealing, creating cDNA. Each step of this process is heat dependent and is therefore done by a thermocycles. As cDNA does not disintegrate as rapidly as RNA, the cDNA can be stored at -20 °C for months.

With the cDNA, qPCR can be performed. First, the cDNA is denatured to allow for annealing. Afterwards, the strands separate, having created two copies of an identical cDNA strand. This process is repeated 20-40 times for the purpose of creating enough cDNA for detection. In qPCR, fluorescent markers bind to specific gene strands in the cDNA. The fluorescence is measured and can be compared to measured fluorescence in other samples. qPCR is therefore highly qualified to compare between samples. [55]

Methods

RNA isolation

This protocol has been adapted from the RNeasy Mini kit from Qiagen.

- Add 350 μL RLT buffer to each sample and slowly pipet up and down to lysate the cells. Gather the RLT buffer with cells.
- Add 350 μL pure ethanol to the RLT buffer and mix well by pipetting.
- Transfer the 700 μL to an RNeasy Mini spin column placed in a 2 mL collection tube.
- Centrifuge this with the eppendorf Centrifuge 5810 R for 15 sec at >8000 g and discard the flow through.
- Add 700 μL Buffer RW1 to the spin column.
- Centrifuge this for 15 sec at >8000 g and discard the flow through.
- Add 500 μL Buffer RPE (with ethanol) to the spin column.
- Centrifuge this for 15 sec at >8000 g and discard the flow through.
- Add 500 μL BufferRPE (with ethanol) to the spin column.
- Centrifuge this for 2 min at >8000 g and discard the flow through.
- To dry the membrane centrifuge the spin column again for 1 min at >8000 g and discard the flow through.
- Place the RNeasy spin column in a new 1.5 mL collection tube, the 2 mL collection tube can be discarded.
- Add 30 μL RNase-free water to the spin column.
- Centrifuge this for 1 min at >8000 g to elute the RNA.
- When the expected RNA yield is low, the previous 2 steps can be repeated with the eluate obtained.

cDNA formation

- First measure the amount of RNA in ng/mL in each sample with a nanodrop:

  - Clean the nanodrop.
  - Measure a blank sample.
  - Measure each sample twice, be sure to wipe the nanodrop between samples.
  - Calculate the average.
- Compensate to make sure each sample has the same amount of RNA by mixing variable amount of RNA template and nuclease-free water till 15 μL in a small tube.
- Add 4 μL 5x iScript Reaction Mix and 1 μL iScript Reverse Transcriptase.
- Incubate the tubes in a MJ Mini^TM Personal Thermal Cycler with the following protocol:
  - 5 minutes at 25 °C.
  - 20 minutes at 46 °C.
  - 1 minute at 95 °C.
  - Store at 4 °C

This protocol is obtained from the iScript cDNA Synthesis Kit.

Performing the qPCR This protocol has been adapted from a protocol written, but unpublished, by Karlijn Slutter, based on a version of Verena Schwach, a version of which can be found on Benchling.

- First, thaw the primers on ice.
- Dilute cDNA with RNase free water in a 1:16 concentration (285 μL water + 19 μL cDNA).
- Dilute each primers to be used with RNase free water in a 1:10 concentration (90 μL water + 10 μL primer). These dilutions can be stored at -20 °C and reused.
- Prepare the Mastermix, take into account that each sample will be measured in triplo and that each primer will have a negative control (also in triplo), according to the following amounts:
  - For each well add 5 μL SensiMix SYBR & Fluorescein Mix.
  - For each well add 0.5 μL Forward Primer.
  - For each well add 0.5 μL Reverse Primer.
- Take a 384 qPCR plate, remember not to talk in front of the plate to inhibit the chance of contamination.
- Add 6 μL mastermix to each well.
- Add 4 μL cDNA to each well or RNase free water to each negative control
- Cover the plate with a foil and make sure it sticks well to the plate with a Film Sealing Roller. Make sure not to touch the foil.
- Spin the plate for 30-60 seconds at 3000 g with the eppendorf Centrifuge 5424 R until air bubbles are gone.
- Place the plate in the CFX384 Touch^TM Real-Time PCR Detection System and enter the following protocol:
  1. 10 minutes at 95 °C.
  2. 15 seconds at 95 °C.
  3. 15 seconds at 60 °C.
  4. 15 seconds at 72 °C.
  5. Repeat step 2 for 39 times.
  6. Add a melt curve from 65 degrees to 95 °C, with steps of 0.5 degrees.
  7. End at 4 °C 'forever', to keep the plate cool till further use.
- The plate can be used for gel electrophoresis, which was not performed in this master thesis, instead the plate was thrown.
- The qPCR should be repeated 3 times to compensate for technical errors, such as pipetting errors.
- Analyze the qPCR data to be able to compare the different samples.

4.2.4 Cx43 protein expression visualized by immunostaining

Theory

Though the general theory behind immunostaining is similar to the theory of 'regular' staining, there are definite differences. Most importantly, immunostaining is an antibody staining and is thus used for the staining of specific proteins. For immunostaining both a primary and secondary antibody are required. The primary antibody is non fluorescent and is generally produced in an animal host. The primary antibody is specific for a certain protein. The secondary antibody is fluorescent, produced in a different animal host than the primary antibody and is specific for all antibodies of the primary antibody animal host. Thus, by adding both the primary and secondary antibody to a tissue sample, the specific protein is labeled with the primary antibody, which is labeled with the secondary antibody, including a fluorescent marker, allowing for the specific protein to be visualized under a fluorescent microscope.

The potential for a certain protein to be expressed is determined with qPCR by measuring the RNA expression for the production protein, whereas the actual expression of these proteins is obtained with immunostaining.

Methods

For the immunostaining, like the regular staining, less washing steps than in the original protocol will be performed.

To stain for the protein Cx43, Anti-Connexin-43 antibody produced in rabbit (C6219, ordered from Sigma Aldrich) is used as primary antibody and Alexa Fluor 647 goat anti-rabbit ordered from Thermo Fisher Scientific (order number A21244) as secondary antibody.

If the CM are not fixated before staining, they have to be fixated first, if they are, the first part of the protocol can be skipped.

Cell fixation:

- First perform a quick washing step of the wells with DPBS.
- For the second washing step, leave the DPBS on for 5 minutes before aspirating.
- Fixate cells by using 200 μL 4% Formaldehyde per well (incubate for 15 minutes)
- Perform a quick washing step of the wells with DPBS.
- For the next washing step, leave the DPBS on for 5 minutes before aspirating.
- At this point the cells can be stored in PBS for one week in the fridge or continue with the cell

Next, the cells need to be permealized for the antibodies to be able to permeate the cell membrane.

Cell permeabilization:

- Wash the cells with DPBS and leave it on for 5 miutes before aspirating.
- Pipet 200 μL 0.1% Triton in each well and incubate for 8 minutes.
- Perform a quick washing step of the wells with DPBS.
- For the next washing step, leave the DPBS on for 5 minutes before aspirating.
- Pipet 200 μL 10% FBS in each well and incubate for 1 hour. This is the blocking step to prevent aspecific binding of the antibody.
- During this hour, dilute the primary antibody to the desired concentration. The Cx43 primary antibody is diluted 1:2000
- Aspirate the FBS.
- Pipet 200 μL primary antibody solution in each well and incubate overnight at 4 °C.
- Perform a quick washing step of the wells with DPBS.
- For the next washing step, leave the DPBS on for 5 minutes before aspirating.
- During the last washing step, dilute the secondary antibody to the desired concentration. The Alexa Fluor 647 anti-rabbit secondary antibody was diluted 1:500. Watch out for exposure to light as much as possible.
- Pipet 200 μL secondary antibody solution in each well and incubate for at least 90 minutes.

- Perform a quick washing step of the wells with DPBS.
- For the next washing step, leave the DPBS on for 5 minutes before aspirating.
- During the last washing step, dilute Hoechst to the desired concentration, for which 1:1000 was used.
- Pipet 200 μL Hoechst solution in each well and incubate for 15 to 30 minutes
- Perform a quick washing step of the wells with DPBS.
- For the next washing step, leave the DPBS on for 5 minutes before aspirating.
- The immunostained wells can now be kept in 4 °C for a few days, as long as they are protected from light.
- In this master thesis the samples have been mounted to a glass slide with prolong gold and visualized under the Nikon Confocal Fluorescence Microscope.

Chapter 5

Results and discussion

5.1 Gel Characteristics

5.1.1 Viscoelastic properties

Figure 5.1 shows the results of the Rheology experiment, as the storage modulus is the same as the Young's modulus, it has been named the Young's modulus here. On the x-axis the different conditions are shown, on the y-axis the Young's modulus is shown in Pa. As each condition was measured with n=3, the standard deviation of each condition is shown as an error margin.

As MWCNTs are sheets of carbon atoms with extremely strong molecular bonds, see subsection 2.2.1, it was expected that the presence of MWCNTs in the GelTA would increase the Young's modulus. However, from the rheology results, it becomes clear that the Young's modulus decreases with GelTA with 0.5, 1, 2 and 3 mg/mL MCWNT compared to pristine GelTA.

As GelTA is a polymer, the Young's modulus is determined by the stress/strain response of the bonds between the polymer strands. It is hypothesized that the initial decrease in Young's modulus is due to the bonds between the GelTA strands and the MWCNTs being weaker than the bonds between the GelTA strands. With low amounts of MWCNTs the strong bonds between the carbon atoms in the MWCNTs then would possibly not make up for the weaker bonds between the MWCNTs and the GelTA strands, causing the Young's modulus to decrease. This is supported by results which show an increase in Young's modulus with the increase in MWCNTs. From 4 mg/mL MWCNts in the GelTA, the strong bonds between carbon atoms make up for the weaker hydrogen bonds between MWCNTs and GelTA polymer strands, causing the Young's modulus from 4 mg/mL MWCNTs in the GelTA onward to be higher than the Young's modulus of the GelTA. The Young's modulus is seen to have a dip at 6 mg/mL MWCNTs in the GelTA. This can be caused by insufficient curing of the hydrogel due to not enough time having been given to these samples before submerging them in DPBS or another measurement error. The difference in Young's modulus between 8 and 9 mg/mL is not high, suggestion that a plateau has been reached, where the increase in MWCNT amount does not increase the Young's modulus.

The Young's modulus of cardiac tissue is 5-10 kPa [48], whereas the measured Young's modulus here does not exceed 2.1 kPa, not even half the value of cardiac tissue. Therefore, when only considering the Young's modulus, this hydrogel is not ideal to mimic the characteristics of human cardiac tissue. Changing the percentage of GelTA could change the Young's modulus to make it more ideal, though the observed higher attachment of the CM to 7.5% GelTA, as discussed in subsection 3.2.4, should be taken into account when changing the GelTA percentage of the scaffolds.

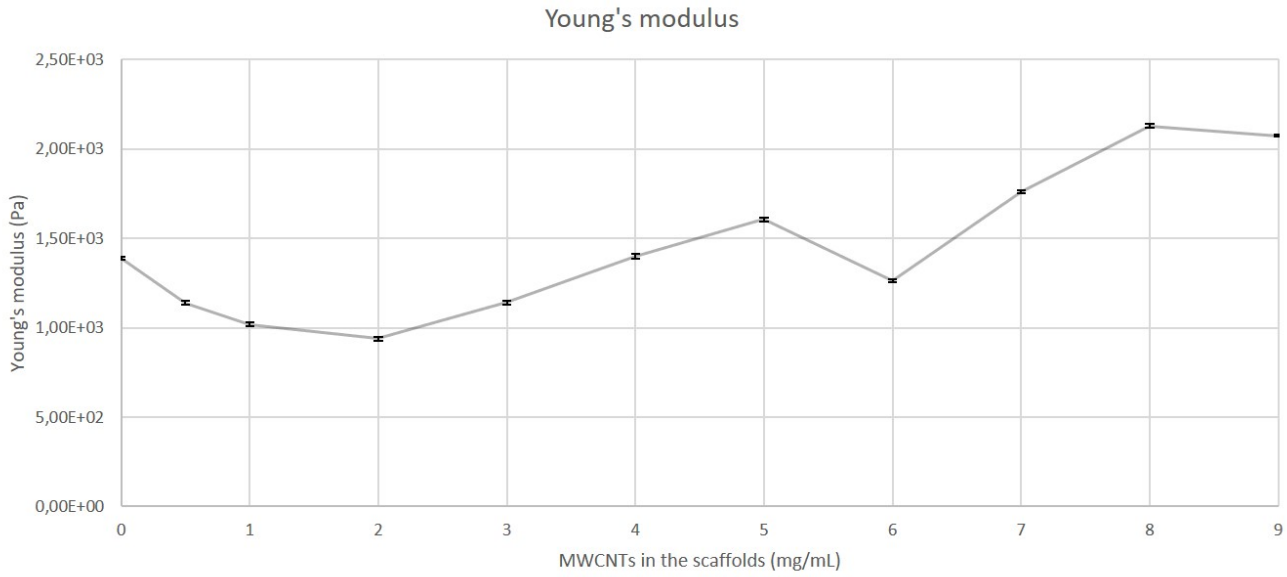

Figure 5.1: **Young's modulus**, The Young's modulus is shown as a function of the amount of MWCNTs present in the scaffolds, for n=3 repetitive measurements.

5.1.2 Conductivity

The results of the four point probe measurement are shown in Figure 5.2, where the impedance, which is the inverse of conductance, is plotted against the frequency.

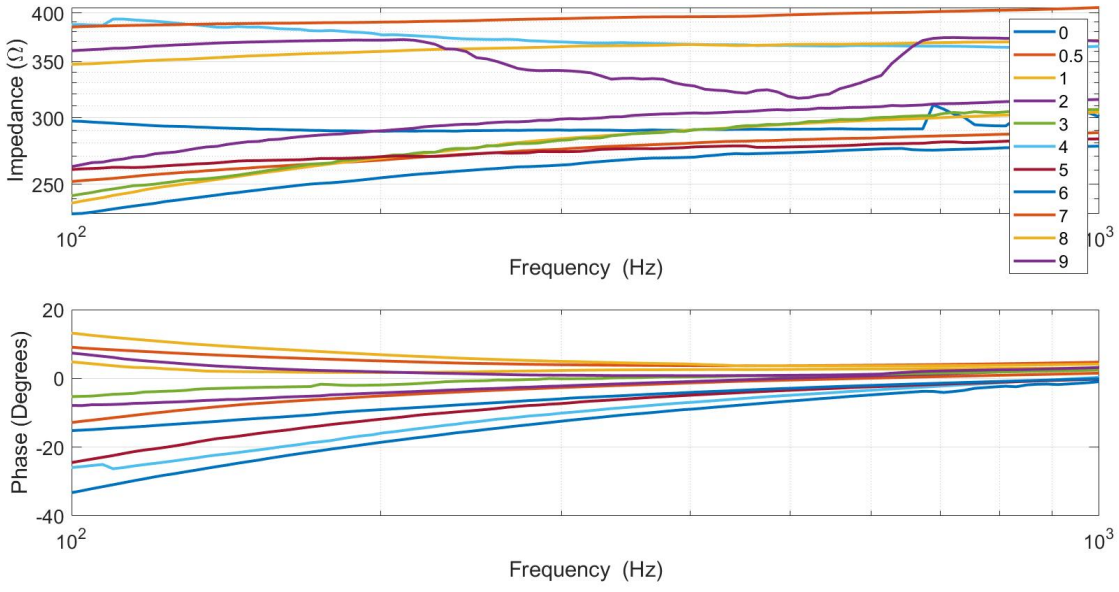

Figure 5.2: **Impedance of the measured hydrogels**. (top) Impedance as a function of the frequency. (bottom) Phase as a function of the frequency. At phase 0, the gel is completely resistive, meaning only the resistance properties of the gel are measured. Measurements on the gel were performed twice for all conditions except for 9 mg/ml MWCNTs, with similar results for both measurements.

To analyse the results it is most ideal to compare the impedance of the gels at phase 0, where only the resistance properties of the gel are measured. When phase 0 does not occur in the measurement, the plateau values can be compared, where the phase is closest to 0. As can be seen from the results, the gels with MWCNTs present are both higher in impedance and lower in impedance than pristine GelTA, depending on the amount of MWCNTs. The hypotheses was that the conductivity would increase with the increasing amount of MWCNTs, which would mean that the impedance would be lower. The results shown here refute this hypothesis. A probable cause for this is the absence of a complete network in the gel formed by the carbon nanotubes. Therefore, through the gel there is a current alternately through MWCNTs and through the GelTA. The current through MWCNTs is electron transport, whereas the current through the gel is ion transport. At low frequencies, the change from electron to ion transport is blocked by the electrical double layer at the interface of the gel and MWCNTs. The electrical double layer acts as a capacitor. [56] Therefore, the MWCNTs present in the gel act as capacitor on low frequencies.

The formation of electrical double layers around the MWCNTs can be neglected when the impedance is measured at frequencies of a MHz level, as the current then passes through the gel fast enough for the electrical double layers to not have an effect anymore. This can be seen from the following Equation 5.1 [57]. At a high frequency, the frequency dependent factor, ω, is high, meaning the impedance is low and can become negligible.

$$Z = \frac{1}{j\omega C} \tag{5.1}$$

This would explain why Su Ryon Shin, et al, 2013 did measure a difference in conductivity between the gels as she measured the conductivity of the hydrogels at a MHz range [21]. As CM contract at Hz range, the range from Hz to kHz, and therefore the measured conductivity of the hydrogels, has been deemed more biologically relevant.

To calibrate the set-up, conductivity standards have been measured, based on values found in literature [58]. Highly conductive sea water has also been measured, which gave a value of around 24 Ω, showing a difference in order of magnitude between the measured conductive sea water and the measured gel samples. This suggests a degree of accuracy of the set-up.

5.2 Cell Characteristics

To obtain a reliable result, multiple runs with DRRAGN CM dissociated from different passages have been performed. The shown results are either the mean of the results of all measurements, or a single representative measurement result is shown, as indicated for each individual figure.

First the general cell characteristics will be discussed, being the cell viability and the contractility of the CM, after which characteristics related to maturity will be discussed.

5.2.1 Viability staining

Figure 5.3 shows how the program CellProfiler 3.1.8 identified the primary objects, with Figure 5.3 (a) showing all stained nuclei and Figure 5.3 (b) showing only the dead stained nuclei. Figure 5.4 shows the calculated viability, based on the results as obtained with Cell Profiler. The viability is defined as the percentage of viable cells of the total of cells, calculated by: Viability=1-(Dead/Nuclei).

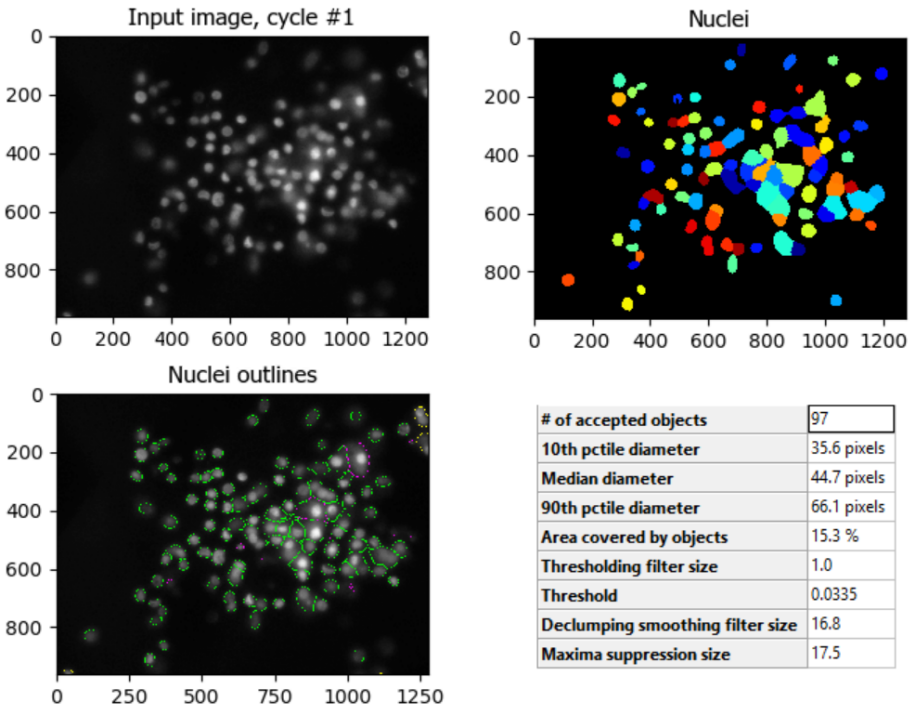

# of accepted objects	97
10th pctile diameter	35.6 pixels
Median diameter	44.7 pixels
90th pctile diameter	66.1 pixels
Area covered by objects	15.3 %
Thresholding filter size	1.0
Threshold	0.0335
Declumping smoothing filter size	16.8
Maxima suppression size	17.5

(a)

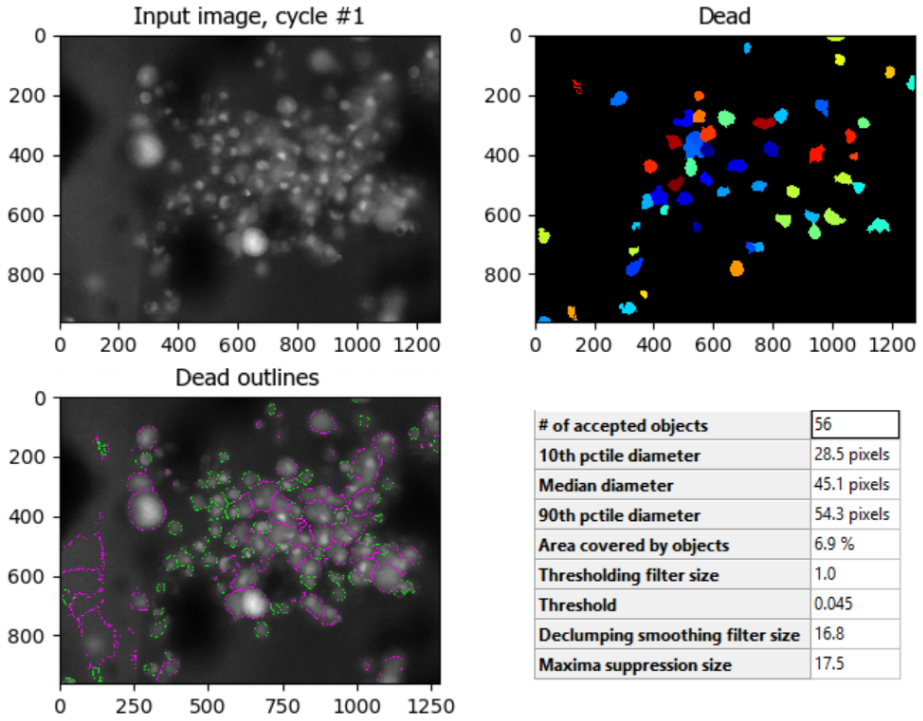

# of accepted objects	56
10th pctile diameter	28.5 pixels
Median diameter	45.1 pixels
90th pctile diameter	54.3 pixels
Area covered by objects	6.9 %
Thresholding filter size	1.0
Threshold	0.045
Declumping smoothing filter size	16.8
Maxima suppression size	17.5

(b)

Figure 5.3: **Identifying of primary objects**. (a) Nuclei of all CM, stained by Hoechst, analyzed with CellProfiler 3.1.8. The top left image shows the picture as seen under the microscope. The bottom left image shows which cells meet the criteria as set in subsection 4.2.1 and are therefore identified as primary objectives. The top right shows the light intensity of each primary object, which can also be set as a criterium for the identifying of the primary objects. This has however not been done in this master thesis. The right left image shows different analyzed values, of which the # of accepted objects is most important, as this is the number of nuclei shown in the image as analyzed by the software. (b) Corresponding nuclei of dead CM, stained with EtdH.

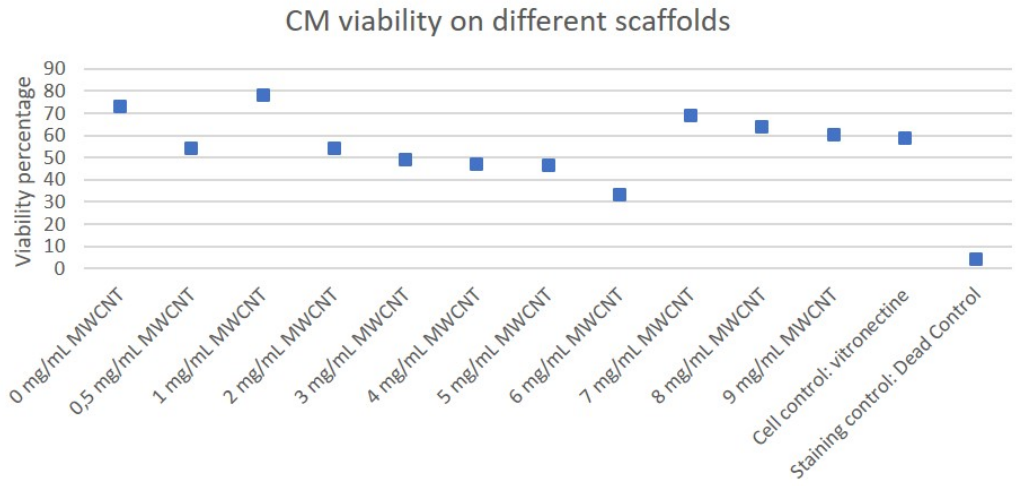

Figure 5.4: **Viability of the scaffolds.** The viability of the different scaffolds as defined by the percentage of viable among the total number of cells, is shown for different MWCNT densities, for a cell control group, CM cultured on vitronectine, and for a staining control group, where all CM have been killed before staining.

As can be seen from Figure 5.3, the viability of the CM decrease with an increase in MWCNTs in the scaffold the CM are cultured on, suggestion that the MWCNTs indeed have a toxic effect on the CM. It has to be assessed whether the decrease in viability due to an increase in MWCNTs is worth a possible increase in maturity of the CM. The very low viability of CM in the staining control show that the staining and analysis are veracious, as the dead cells are indeed labeled as dead.

5.2.2 Contractility

The most important characteristics of contractility, being the contractility rate (beats/min), the maximum contraction velocity (μm/sec) and the maximum relaxation velocity (μm/sec) are shown in Table 5.1. They have been measured after the CM have been in culture for 11 days. The average of n=6 is shown.

Scaffolds of 7.5% GelTA, with	Contractility rate (beats/min)	Maximum contraction velocity (μm/sec)	Maximum relaxation velocity (μm/sec)
0 mg/mL MWCNTs	32.2	5.0	4.9
1 mg/mL MWCNTs	39.6	3.4	3.2
3 mg/mL MWCNTs	46.1	1.2	1.3
5 mg/mL MWCNTs	46.3	1.7	1.6
7 mg/mL MWCNTs	47.9	3.6	3.6
9 mg/mL MWCNTs	36.8	5.1	5.2

Table 5.1: **Contractility characteristics.** The measured average contractility rate (beats/min), the average maximum contraction velocity (μm/sec) and the average maximum relaxation velocity (μm/sec) of n=9 are shown for each condition.

From these results it can be seen that there is an increase in contractility rate upon the addition of MWCNTs to the GelTA scaffolds. It can by hypothesized that this increase contractility rate is due to an increase in cell-cell coupling due to the presence MWCNT. It would be possible that due to the increased cell-cell coupling, the CM are able to react more to their neighboring CM. Therefore more CM would

be able to follow the same CM, which would be the fastest contracting CM. The MWCNT could also hypothetically increase the conduction velocity, also leading to an increase in contractility rate.

To validate this hypothesis more research is required.

5.2.3 RNA expression of the gene encoding for Cx43 protein from qPCR

A qPCR run has been performed with multiple samples, cultured in multiple runs. The RNA expression of each sample is shown relative to the control. In each sample, the control is the RNA expression in the CM cultured on pristine GelTA from that run. In other words, the RNA expression in the control samples, is set to 1. The RNA expression is shown both as an average relative expression and the relative expression per performed run.

The qPCR results are expected to show an increase in RNA expression of the gene encoding for Cx43 with an increase in scaffold conductivity, due to maturity of the CM. However, as the scaffold does not increase in conductivity, these results were not expected to be shown in the RNA expression related to an increase in MWNCTs in the scaffold.

The results are shown relative to the control group, which is the RNA expression of the gene encoding for Cx43 of CM cultured on pristine GelTA. The HouseHold gene used, hARP has a δ Ct of 1 cycle with most samples per run. In a few samples the δ Ct is higher than 1 per run, which is probably due to pipetting errors. These samples have therefore been excluded from analysis. The other samples can be compared to each other.

There is no real difference in RNA expression of the gene encoding for Cx43 relative to the control group of CM cultured on pristine GelTA shown in CM cultured on GelTA with 3 mg/mL MWCNT, meaning the fold change is around 1. It is possible that this amount of MWCNT is too low to have an effect on the maturity of CM.

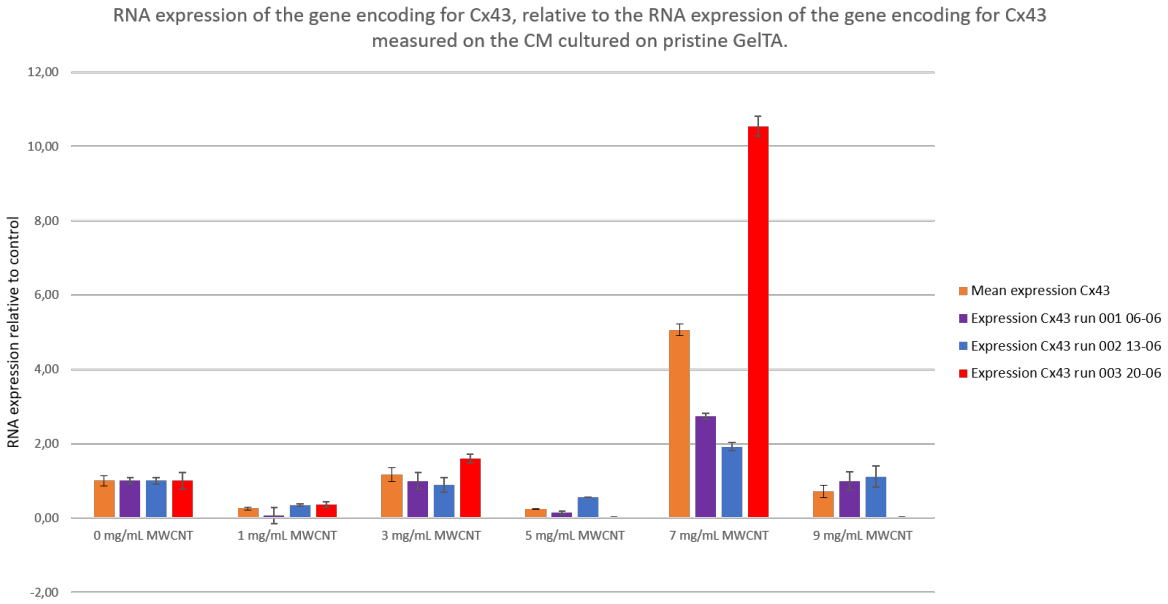

Figure 5.5: **Mean expression of the gene encoding for Cx43.** The RNA expression of the gene encoding for Cx43 relative to the control group, defined as RNA expression of the CM cultured on pristine 7.5 % GelTA. The gene expression is averaged over n=2.3 samples per dissociation runs. Ideally, all these results should be identical. Therefore, the standard deviation between all results is indicated. The results are ordered by increasing MWCNT density in the gel layers. Both the mean relative expression and the relative expression of each separate run are shown.

The RNA expression of the gene encoding for Cx43 in CM cultured on GelTA with 7 mg/mL MWCNT relative to the control group of CM cultured on pristine GelTA is high, meaning there is a positive fold change. It is possible that this increase is due to the presence of MWCNT, which could increase the maturity of the CM.

The RNA expression of the gene encoding for Cx43 in CM cultured on GelTA with 1, 5 and 9 mg/mL relative to the control group of CM cultured on pristine GelTA shown is low, meaning there is a negative fold change. This can be due to negative effects on the maturity of CM due to the presence of MWCNT.

It is unknown why the presence of MWCNT seems to have both a positive and a negative fold change on the RNA expression of the gene encoding for Cx43 relative to the control group of CM cultured on pristine GelTA. Further research is needed to explain these results.

5.2.4 Cx43 protein expression visualized by immunostaining

An immunostaining has been performed on each condition with n=7, a representative image of which is shown here. Figure 5.6 shows the results for the immunostaining of the CM cultured on pristine 7.5% GelTA and 7.5% GelTA with 1 and 3 mg/mL MWCNT. Figure 5.7 shows the results for the immunostaining of the CM cultured on 7.5% GelTA with 5, 7 and 9 mg/mL MWCNT. For immunostaining, images are made from different channels, showing different aspects of the cells. Here, images are shown both with all channels merged and all channels seperately.

For people suffering from deutan color vision deficiency, the images with the merged channels are shown in different colors in section A.2.

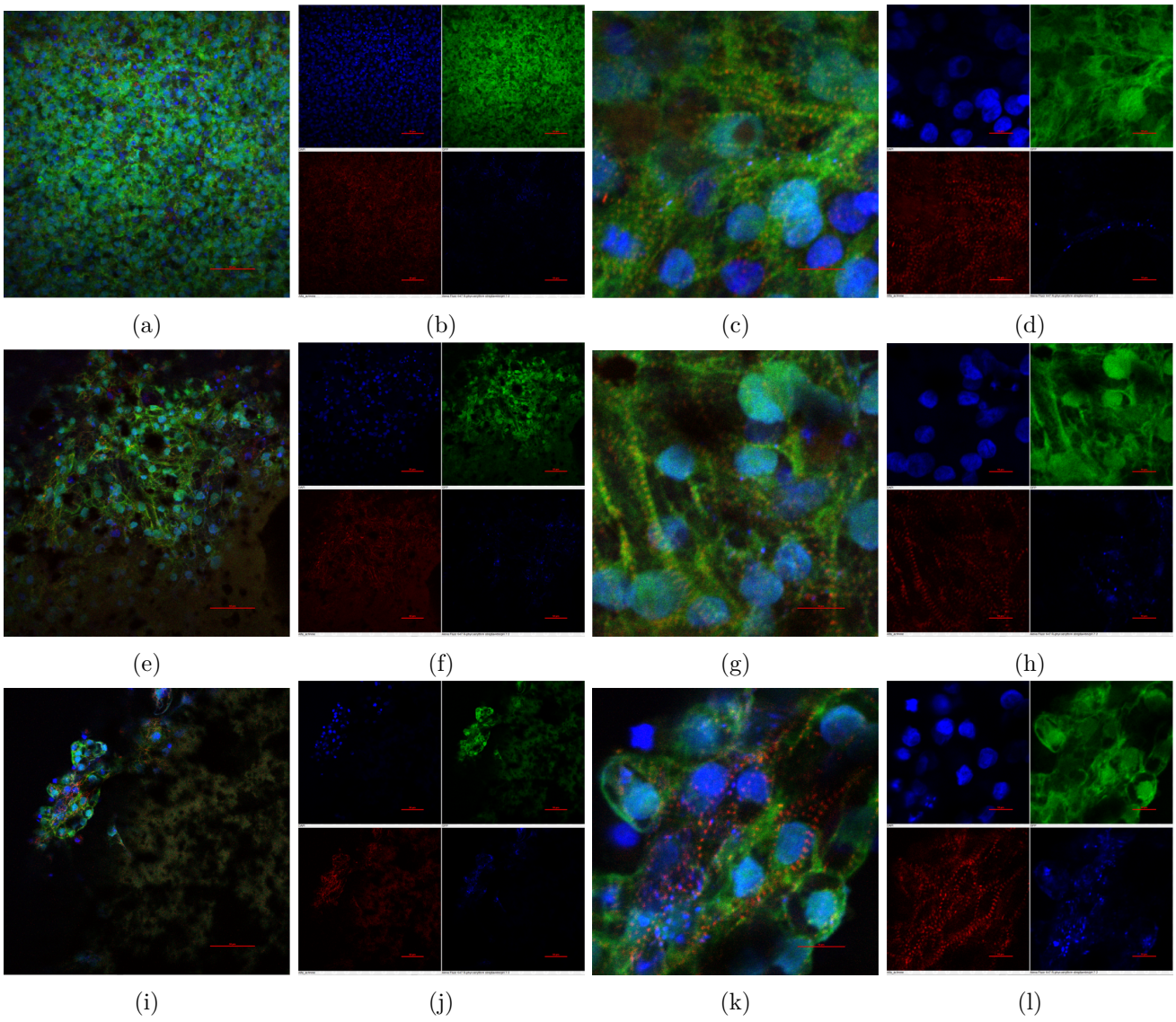

Figure 5.6: **Immunostaining results 0, 1 and 3 mg/mL MWCNT**. Images (a), (c), (e), (g), (i), (k) show the merger of the DAPI channel, the GFP channel, the α-actinine channel and the Alexa Fluor 647 channel, whereas images (b), (d), (f), (h), (j), (k) show each channel separately. Here the DAPI channel (top left) shows the stained nuclei, the GFP channel (top right) shows the binding of GFP to Nkx2.5, a marker for cardiac differentiation, the α-actinine channel (bottom left) shows the mRubyII bound to α-actinine and the Alexa Fluor 647 channel (bottom right) shows the stained Cx43 protein. (a), (b), (c) and (d) show the results from the CM cultured on pristine 7.5% GelTA, with (a) and (b) taken at 40x magnification, with the scale bar at 50 μm, and (c) and (d) at a magnification of 5.29 of the 40x magnified image, with the scale bar at 10 μm. Images (e), (f), (g) and (h) show the results from the CM cultured on 7.5% GelTA with 1 mg/mL MWCNT, with (e) and (f) taken at 40x magnification, with the scale bar at 50 μm, and (g) and (h) at a magnification of 5.29 of the 40x magnified image, with the scale bar at 10 μm. Images (i) (j) (k) and (l) show the results from the CM cultured on 7.5% GelTA with 3 mg/mL MWCNT, with (i) and (j) taken at 40x magnification, with the scale bar at 50 μm, and (k) and (l) at a magnification of 5.29 of the 40x magnified image, with the scale bar at 10 μm. For each condition n=7 experiments have been performed, from which a representative image has been shown here.

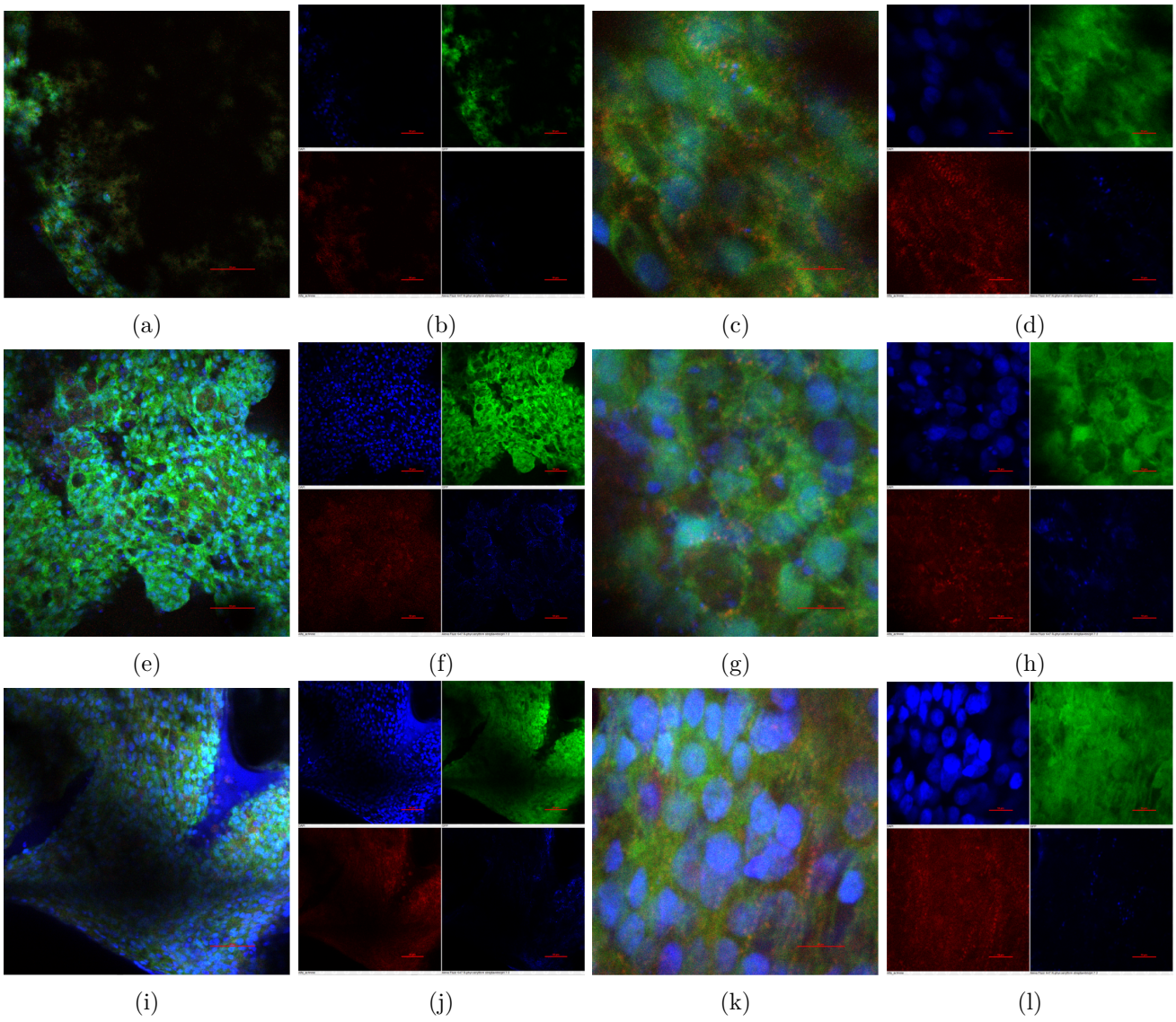

Figure 5.7: **Immunostaining results 5, 7 and 9 mg/mL MWCNT**. Images (a), (c), (e), (g), (i), (k) show the merger of the DAPI channel, the GFP channel, the α-actinine channel and the Alexa Fluor 647 channel, whereas images (b), (d), (f), (h), (j), (k) show each channel separately. Here the DAPI channel (top left) shows the stained nuclei, the GFP channel (top right) shows the binding of GFP to Nkx2.5, a marker for cardiac differentiation, the α-actinine channel (bottom left) shows the mRubyII bound to α-actinine and the Alexa Fluor 647 channel (bottom right) shows the stained Cx43 protein. (a), (b), (c) and (d) show the results from the CM cultured on 7.5% GelTA with 5 mg/mL MWCNT, with (a) and (b) taken at 40x magnification, with the scale bar at 50 μm, and (c) and (d) at a magnification of 5.29 of the 40x magnified image, with the scale bar at 10 μm. Images (e), (f), (g) and (h) show the results from the CM cultured on 7.5% GelTA with 7 mg/mL MWCNT, with (e) and (f) taken at 40x magnification, with the scale bar at 50 μm, and (g) and (h) at a magnification of 5.29 of the 40x magnified image, with the scale bar at 10 μm. Images (i) (j) (k) and (l) show the results from the CM cultured on 7.5% GelTA with 9 mg/mL MWCNT, with (i) and (j) taken at 40x magnification, with the scale bar at 50 μm, and (k) and (l) at a magnification of 5.29 of the 40x magnified image, with the scale bar at 10 μm. For each condition n=7 and the most representative image has been shown here.

Cx43

The immunostaining results show a trend similar to the qPCR results, showing that not only do the CM have a higher RNA expression of the gene encoding for the Cx43 protein, but the expression of the Cx43 protein itself is also increased. It can be seen that the Cx43 expression in the CM cultured on pristine 7.5% GelTA is present, though minor, similar to the CM cultured on 1 mg/mL MWCNT in the GelTA. The CM cultured on 3 mg/mL showed a high Cx43 expression compared to pristine GelTA, despite the similar possibility for Cx43 expression. The CM cultured on 7 mg/mL MWCNT in GelTA show a very high Cx43 expression, similar to the trend shown in the qPCT results. Similar to the qPCR results, the CM cultured on 5 and 9 mg/mL MWCNT in the GelTA showed low expressions of Cx43. When looking at maturity however, it is more important to look at the whether the distribution of the Cx43 protein is homogeneous than the amount of protein which is present, as the Cx43 is expressed in the gap junctions. These gap junctions regulate the cell-cell coupling and thereby the contractility. A more homogeneous distribution of the Cx43 would therefore entail a more homogeneous distribution of gap junctions and cell-cell coupling. As the CM have been cultured in a monolayer like fashion with multiple cells stacked on top of each other, it is hard to draw a strong conclusion with regard to the Cx43 distribution based on Figure 5.6 and Figure 5.7.

A way to analyze the Cx43 distribution would be to culture the CM as described in this master thesis, but before analysis the CM should then be reseeded as single cells to determine the single cell characteristics.

α-actinine

As discussed in section 2.4, the organization of the α-actinine strands within a CM is a sign for maturity. The α-actinine strands seem to be disorganized in the CM cultured on pristine GelTA and the CM cultured on scaffolds with 1 mg/mL MWCNTs. The α-actinine strands are more organized in CM cultured on scaffolds with 3, 5 and 9 mg/mL MWCNTs. As the α-actinine are not separately visible in the CM cultured on 7 mg/mL MWCNTs, the organization cannot be discussed, however following the previously discussed results where the CM cultured on 7 mg/mL MWCNTs showed signs of maturity, the expectation is that this is similar with regard to the organization of the α-actinine strands.

However, as the CM have been cultured in a monolayer like fashion with multiple cells stacked on top of each other, it is hard to draw a strong conclusion with regard to the α-actinine organization based on Figure 5.6 and Figure 5.7, as it is hard to determine which sarcomere belongs to which cell. It is therefore not possible to analyse the sarcomere orientation in each separate cell.

A way to analyze the allignment of the sarcomere structures would be to culture the CM as described in this master thesis, but before analysis the CM should then be reseeded as single cells to determine the single cell characteristics.

Chapter 6

Conclusion

This work describes the influence of a conductive hydrogel on the maturation of CM with respect to using a non-conductive hydrogel. This work starts with the process on how a model has been developed to assess these differences in maturity. CM cultured on scaffolds with different densities of MWCNTs have been assessed for multiple maturation characteristics.

It was found that the CM cultured on scaffolds with different amounts of MWCNTs present showed an increase in certain maturity characteristics when compared to CM cultured on pristine GelTA. Where the relative gene expression of Cx43, same as the Cx43 protein expression, was elevated in the CM cultured on GelTA with 7 mg/mL, the α-actinine strands seemed slightly more organized in CM cultured on scaffolds with 3, 5 and 9 mg/mL MWCNTs. However, both the relative gene expression of Cx43 and the organization of the α-actinine strands shown in this master thesis cannot give an accurate conclusion regarding the maturity. Single cell analysis regarding the distribution of the Cx43 protein expression and the organization of α-actinine strands should be performed to give a more definitive conclusion.

Additionaly, since the conductivity of the different hydrogel scaffolds did not increase with the presence of MWCNTs, the differences found in the maturity of the CM cultured on the different scaffolds cannot be related to the conductivity of the scaffolds. It is however possible that the conductivity of the scaffolds does increase locally, at the places in the scaffold where the MWCNTs are present and form a network. As the CM do not always spread across the entire scaffolds but are locally attached, this possible local increase in conductivity could increase the maturity of these CM, as is in correspondence with the presented results. Whether and where the MWCNTs have formed local networks can be anylsed with a CryoTEM.

More research is necessary to either support or rebut this theory. In chapter 7 possible improvements to the scaffolds designed in this master thesis and the experiments done here, are explained.

Chapter 7

Future outlook and recommendations

In this chapter, recommendations are given on improving the scaffolds designed during this master thesis, with as ultimate goal the creation of mature CM in 3D.

7.1 Improving scaffold conductivity

As explained in subsection 5.1.2, the absence of improvement with regard to the conductivity of the scaffolds is likely due to the absence of a network formed by the MWCNTs. By applying an electric field over the scaffold during curing, the MWCNTs will start aligning, which will create a MWCNT network through the scaffolds, which should theoretically increase the conductivity of the scaffolds. [59] Whether the application of an electric field indeed aligns the MWCNTs to form a network can be assessed with a CryoTEM.

7.2 Mold for reproducible fabrication of thin hydrogel layers

While performing the rheology experiments, thin hydrogel layers were formed rather easily and very reproducible. The mold used for the rheology experiments, shown in Figure 4.1, has as thickness of 1.5 μ. However but by having a mold of 0.5 μm manufactured and placing a coated glass slide on top of the mold, a facile, reproducible method for the production of homogeneously thick hydrogel layers would be developed. As the different gels are all in contact with each other to allow for the hydrogel to be pipetted into the mold, pacing could also be applied to this concept. By making an extra gels on both sides and placing pacers in these extra gels, the hydrogels within could experience the pacing and therefore form a MWCNT network.

7.3 Maturity assessment

From this report is has become clear that no decisive conclusions could be drawn with regard to the maturity due to the monolayer like fashion in which the CM have been cultured. A different way to assess the maturity would be to first culture the CM in this monolayer fashion for a length of time, followed by dissociation of the CM reseeding of the CM as single cells, to characterize the single cell characteristics.

It is also possible to use different maturity parameters, such as investigating which metabolic substrate the CM use. Immature CM use glucose as a metabolic substrate, whereas mature CM use fatty acids. [4] This can be examined by measuring the amount of lactate generated by the CM. [60]

Another maturity characteristic which has not been looked into, is the drug response of the cultured CM. The contraction frequency of mature CM increases upon addition of a positive inotrope, such as isoprenaline. [61] As one of the goals of culturing mature CM is to create a platform of CM for the evaluation of drug response, the drug response of the CM as a measurement of maturity can bring valuable information.

7.4 hiPSC-CM

There are many advantages of using human induced Pluripotent Stem Cell derived CM (hiPSC-CM) instead of Embryonic Stem Cell derived CM, which have been used in this master thesis. One of these advantages is that hiPSC derived CM can create patient specific disease models. This can be beneficial to test patient specific health care. It is therefore recommended to repeat the performed experiments, preferably in combination with the other suggested recommendations, with hiPSC-CM to assess the maturity characteristics of hiPSC-CM cultured on conductive scaffolds. [62]

7.5 3D

As stated in subsection 3.2.6, a migration is visible in CM cultured in a 3D cardiac model obtained via an aqueous two-phase system of GelTA and PEO. As this migration however was not sufficient to form a network where all CM have cell-cell contact, it is recommended to repeat these experiments with either different GelTA:PEO ratios, a different PEO percentage or a higher molecular weight of the PEO, or a combination of the three.

Appendix A

Appendix

A.1 Appendix 1 GelMA Fabriacation protocol

Preparation of GelMA with an expected 96% degree of methacrylation.
Day 0:

- Prepare 0.25 M CB buffer by dissolving 7,95 g sodium carbonate and 14,65 g sodium bicarbonate in 1 L distilled water.
- Take 5 g Gelatin Porcine Skin, add 50 mL CB-buffer (sterile) in a cleaned Erlenmeyer flask with a magnet.
- Set undisolved mixture in a water bath on heating plate, let it rotate (240rpm) at 50 °C until Gelatin is dissolved (this can take as little as 10 minutes). Cover Erlenmeyer flask with aluminum foil. Check for temperature with a mercury thermometer (indicated temperature on plate will be 100-115 °C).
- When Gelatin is dissolved (uniform solution, no more visible granula), adjust the pH to 9 with HCl. When the pH has reached 9, add 0.5 mL Methacrylic Anhydride (276685-100 mL) dropwise (using a 1000 μL pipette) and let emulsion rotate (240rpm) at 50 °C for 3 hours, covered.
- After 3 hours, readjust the pH to 7.4 to stop the reaction.
- Prepare dialysis membrane (Spectro/Por molecularporous membrane tubing, MWCO 12-14,000, Fisher Scientific) by cutting them in proper sizes and washing them with distilled water to soften them (2 x 20-30 cm should be enough). Close one side of the membrane by clipping on a weighted bag clip.
- Transfer diluted GelMA with a funnel into the dialysis membranes, check for leakage. Close the second end of the membrane by clipping on a non-weighted bag clip. Fill each membrane only around half way, to leave enough space for water to diffuse into the membrane. Make sure to get as much of the air out of the membrane as possible. Check again for leakage!!
- Place the membranes into distilled water in a 5 L plastic beaker.
- Let dialysis run at 40 °C for two hours and change the water, repeat this.
- Then let the dialysis run at least 5 days with magnetic stirrer (500 rpm if possible). Cover the beaker with aluminum foil to prevent cross-linking by visible light. Change water 2 times a day (5 L water need some time to warm up before dialysis is effective, so do it morning and evening). Each time turn/flip upside down 5-6 times the membranes to homogenize the content! (This step removes the toxic unreacted MA, so if more GelMA is dialyzed, consider changing water more often and/or let the step run longer).

Day 5 (or 7):

- Prepare adequate number of 50 mL Falcon tubes, each will contain 25 mL (not more!) of the solution.
- Next steps must be handled fast to maintain the liquid at 40 °C at all time.

- Sterilize the liquidwith a sterile vacuum Express Plus (0.22 μm) Milipore filtration cup to filter the liquid. BE QUICK! If the liquid doesn't filter well, consider diluting it with miliQ water.
- Transfer sterilized polymer into 50 mL-Falcons (25 to 30 mL in each is ideal).
- Drop the tubes into liquid nitrogen until all the liquid is frozen.
- Remove the caps from the tubes and slightly turn them back on. Place 4 tubes into a free-drier pot. Freeze dry the GelMA for at least 3 days.
- Store the freeze dried GelMA at 4 °C.

A.2 Appendix 2 Immunostaining results for people suffering from deutan color vision deficiency

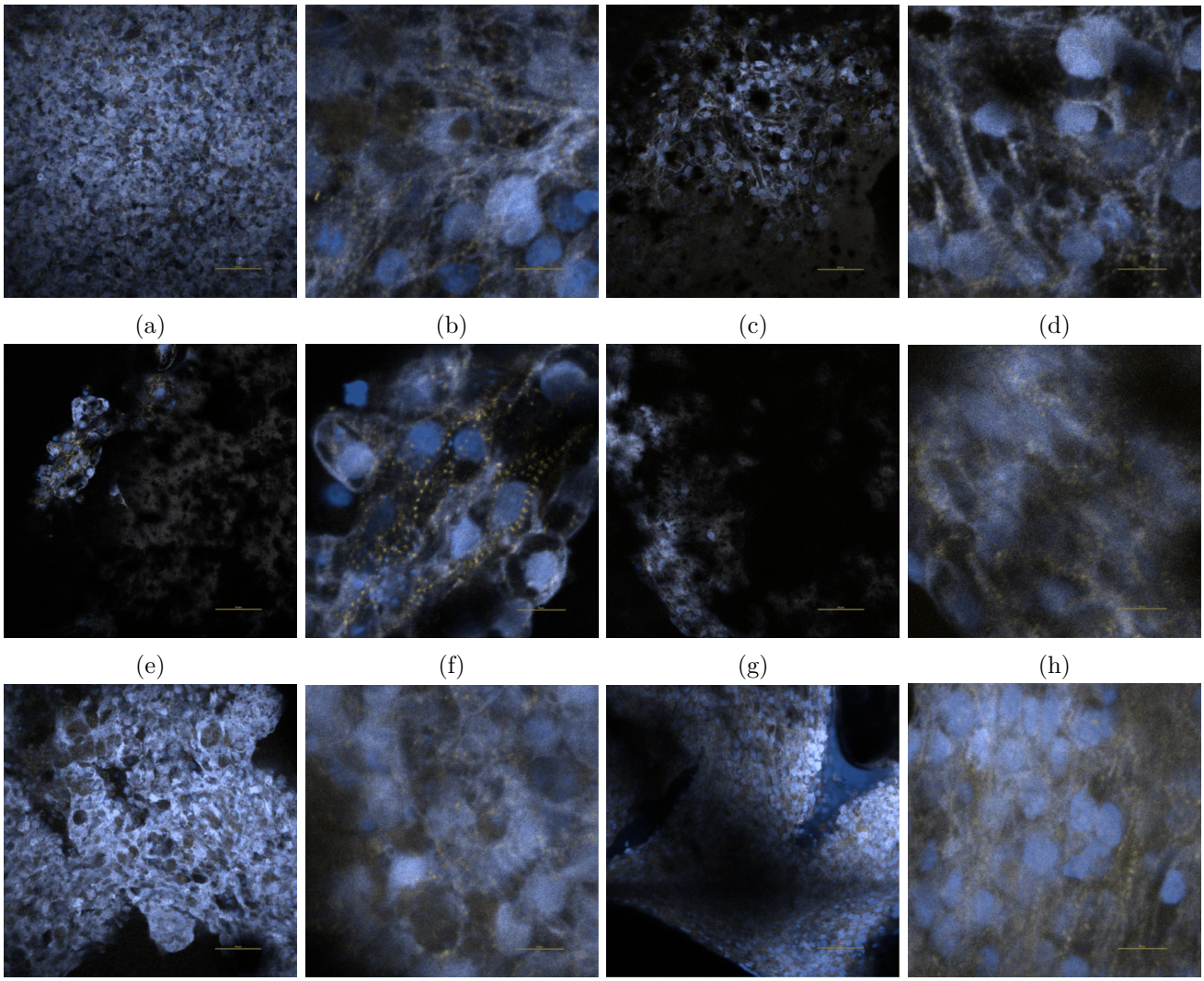

Figure A.1: **Immunostaining results of all merged channels from 0, 1, 3, 5, 7 and 9 mg/mL MWCNT**. (a) Shows the results from pristine 7.5% GelTA taken at 40x magnification. (b) Shows the results from pristine 7.5% GelTA taken at magnification of 5.29 of the 40x magnified image. (c) Shows the results from 7.5% GelTA with 1 mg/mL MWCNT taken at 40x magnification. (d) Shows the results from 7.5% GelTA with 1 mg/mL MWCNT taken at magnification of 5.29 of the 40x magnified image. (e) Shows the results from 7.5% GelTA with 3 mg/mL MWCNT taken at 40x magnification. (f) Shows the results from 7.5% GelTA with 3 mg/mL MWCNT taken at magnification of 5.29 of the 40x magnified image. (g) Shows the results from 7.5% GelTA with 5 mg/mL MWCNT taken at 40x magnification. (h) Shows the results from 7.5% GelTA with 5 mg/mL MWCNT taken at magnification of 5.29 of the 40x magnified image. (i) Shows the results from 7.5% GelTA with 7 mg/mL MWCNT taken at 40x magnification. (j) Shows the results from 7.5% GelTA with 7 mg/mL MWCNT taken at magnification of 5.29 of the 40x magnified image. (k) Shows the results from 7.5% GelTA with 9 mg/mL MWCNT taken at 40x magnification. (l) Shows the results from 7.5% GelTA with 9 mg/mL MWCNT taken at magnification of 5.29 of the 40x magnified image. For each condition n=7 and the most representative image has been shown here. For each image at 40x magnification the scale bar is 50 μm and for the images at 5.29 times the 40x magnification the scale bar is 10 μm.

Bibliography

[1] W. H. Organization 2017.

[2] B. Berkrot, "Success rates for experimental drugs falls: study," 2011.

[3] K. Yue, G. T. de Santiago, M. M. Alvarez, A. Tamayol, N. Annabi, and A. Khademhosseini, "Synthesis, properties, and biomedical applications of gelatin methacryloyl (gelma) hydrogels," *Biomaterials*, vol. 73, pp. 254 – 271, 2015.

[4] X. Yang, L. Pabon, and C. E. Murry, "Engineering adolescence: Maturation of human pluripotent stem cell-derived cardiomyocytes," *Circulation research*, vol. 114, pp. 511–523, 2014.

[5] P. Baei, S. Jalili-Firoozinezhad, S. Rajabi-Zeleti, M. Tafazzoli-Shadpour, H. Baharvand, and N. Aghdami, "Electrically conductive gold nanoparticle-chitosan thermosensitive hydrogels for cardiac tissue engineering," *Materials Science and Engineering: C*, vol. 63, pp. 131 – 141, 2016.

[6] J. L. Drury and D. J. Mooney, "Hydrogels for tissue engineering: scaffold design variables and applications," *Biomaterials*, vol. 24, no. 24, pp. 4337 – 4351, 2003. Synthesis of Biomimetic Polymers.

[7] G. L. Ying, N. Jiang, S. Maharjan, Y. X. Yin, R. R. Chai, X. Cao, J. Z. Yang, A. K. Miri, S. Hassan, and Y. S. Zhang, "Aqueous Two-Phase Emulsion Bioink-Enabled 3D Bioprinting of Porous Hydrogels," *Advanced Materials*, vol. 30, no. 50, pp. 1–9, 2018.

[8] D. Z. Wang, Z. Tian, F. Menard, and K. Kim, "Comparative study of gelatin methacrylate hydrogels from different sources for biofabrication applications," *Biofabrication*, vol. 9, 08 2017.

[9] S. Ahadian, M. Estili, V. J. Surya, J. Ramón-Azcón, X. Liang, H. Shiku, M. Ramalingam, T. Matsue, Y. Sakka, H. Bae, K. Nakajima, Y. Kawazoe, and A. Khademhosseini, "Facile and green production of aqueous graphene dispersions for biomedical applications," *Nanoscale*, vol. 7, pp. 6436–6443, 2015.

[10] M. Sun, X. Sun, Z. Wang, S. Guo, G. Yu, and H. Yang, "Synthesis and Properties of Gelatin Methacryloyl (GelMA) Hydrogels and Their Recent Applications in Load-Bearing Tissue.," *Polymers*, vol. 10, nov 2018.

[11] N. Celikkin, S. Mastrogiacomo, J. Jaroszewicz, X. F. Walboomers, and W. Swieszkowski, "Gelatin methacrylate scaffold for bone tissue engineering: The influence of polymer concentration," *Journal of Biomedical Materials Research Part A*, vol. 106, no. 1, pp. 201–209, 2018.

[12] N. T. B. Linh, C. D. G. Abueva, and B.-T. Lee, "Enzymatic in situ formed hydrogel from gelatin–tyramine and chitosan-4-hydroxylphenyl acetamide for the co-delivery of human adipose-derived stem cells and platelet-derived growth factor towards vascularization," *Biomedical Materials*, vol. 12, p. 015026, feb 2017.

[13] G. Yang, Z. Xiao, X. Ren, H. Long, H. Qian, K. Ma, and Y. Guo, "Enzymatically crosslinked gelatin hydrogel promotes the proliferation of adipose tissue-derived stromal cells.," *PeerJ*, vol. 4, p. e2497, 2016.

[14] K. Park, k. ko, y. k. Joung, H. Shin, and K. Park, "In situ cross-linkable gelatin–poly(ethylene glycol)–tyramine hydrogel via enzyme-mediated reaction for tissue regenerative medicine," *J. Mater. Chem.*, vol. 21, pp. 13180–13187, 08 2011.

[15] S. Sakai, K. Hirose, K. Taguchi, Y. Ogushi, and K. Kawakami, "An injectable, in situ enzymatically gellable, gelatin derivative for drug delivery and tissue engineering," *Biomaterials*, vol. 30, no. 20, pp. 3371 – 3377, 2009.

[16] N. E. Simpson, C. L. Stabler, C. P. Simpson, A. Sambanis, and I. Constantinidis, "The role of the cacl2–guluronic acid interaction on alginate encapsulated βtc3 cells," *Biomaterials*, vol. 25, no. 13, pp. 2603 – 2610, 2004.

[17] S. S. Mihardja, R. E. Sievers, and R. J. Lee, "The effect of polypyrrole on arteriogenesis in an acute rat infarct model," *Biomaterials*, vol. 29, no. 31, pp. 4205 – 4210, 2008.

[18] R. K. Kankala, K. Zhu, X.-N. Sun, C.-G. Liu, S.-B. Wang, and A.-Z. Chen, "Cardiac tissue engineering on the nanoscale," *ACS Biomaterials Science and Engineering*, vol. 4, no. 3, pp. 800–818, 2018.

[19] A. Khan, R. Rashid, G. Murtaza, and A. Zahra, "Gold nanoparticles: Synthesis and applications in drug delivery," *Tropical Journal of Pharmaceutical Research*, vol. 13, pp. 1169–1177, 07 2014.

[20] D. V. Haute and J. M. Berlin, "Challenges in realizing selectivity for nanoparticle biodistribution and clearance: lessons from gold nanoparticles.," *Therapeutic delivery*, vol. 8, pp. 763–774, aug 2017.

[21] S. R. Shin, S. M. Jung, M. Zalabany, K. Kim, P. Zorlutuna, S. bok Kim, M. Nikkhah, M. Khabiry, M. Azize, J. Kong, K.-t. Wan, T. Palacios, M. R. Dokmeci, H. Bae, X. S. Tang, and A. Khademhosseini, "Carbon-Nanotube-Embedded Hydrogel Sheets for Engineering Cardiac Constructs and Bioactuators," *ACS Nano*, vol. 7, pp. 2369–2380, mar 2013.

[22] D. Mohanta, S. Patnaik, S. Sood, and N. Das, "Carbon nanotubes: Evaluation of toxicity at biointerfaces," *Journal of Pharmaceutical Analysis*, 2019.

[23] P. Khalid, V. B. Suman, M. A. Hussain, and A. B. Arun, "Toxicology of carbon nanotubes - A review," *International Journal of Applied Engineering Research*, vol. 11, no. 1, pp. 148–157, 2016.

[24] P. Cherukuri, S. M. Bachilo, S. H. Litovsky, and R. B. Weisman, "Near-infrared fluorescence microscopy of single-walled carbon nanotubes in phagocytic cells," *Journal of the American Chemical Society*, vol. 126, no. 48, pp. 15638–15639, 2004. PMID: 15571374.

[25] S. D. Bird, P. A. Doevendans, M. A. van Rooijen, A. Brutel de la Riviere, R. J. Hassink, R. Passier, and C. L. Mummery, "The human adult cardiomyocyte phenotype," *Cardiovascular Research*, vol. 58, pp. 423–434, may 2003.

[26] S. D. Lundy, W.-Z. Zhu, M. Regnier, and M. A. Laflamme, "Structural and Functional Maturation of Cardiomyocytes Derived from Human Pluripotent Stem Cells," jul 2013.

[27] I. Kehat, D. Kenyagin-Karsenti, M. Snir, H. Segev, M. Amit, A. Gepstein, E. Livne, O. Binah, J. Itskovitz-Eldor, and L. Gepstein, "Human embryonic stem cells can differentiate into myocytes with structural and functional properties of cardiomyocytes," *The Journal of Clinical Investigation*, vol. 108, no. 3, pp. 407–414, 2001.

[28] S. S. Nunes, J. W. Miklas, J. Liu, R. Aschar-Sobbi, Y. Xiao, B. Zhang, J. Jiang, S. Masse, M. Gagliardi, A. Hsieh, N. Thavandiran, M. A. Laflamme, K. Nanthakumar, G. Gross, P. H. Backx, G. Keller, and M. Radisic, "Biowire: a new platform for maturation of human pluripotent stem cell derived cardiomyocytes," aug 2013.

[29] K. Umetani, D. H. Singer, R. McCraty, and M. Atkinson, "Twenty-Four Hour Time Domain Heart Rate Variability and Heart Rate: Relations to Age and Gender Over Nine Decades," *Journal of the American College of Cardiology*, vol. 31, pp. 593 LP – 601, mar 1998.

[30] N. J. Severs, "The cardiac muscle cell," *BioEssays*, vol. 22, no. 2, pp. 188–199, 2000.

[31] J. Hanna, A. W. Cheng, K. Saha, J. Kim, C. J. Lengner, F. Soldner, J. P. Cassady, J. Muffat, B. W. Carey, and R. Jaenisch, "Human embryonic stem cells with biological and epigenetic characteristics similar to those of mouse ESCs," *Proceedings of the National Academy of Sciences*, vol. 107, no. 20, pp. 9222–9227, 2010.

[32] M. Radisic, H. Park, H. Shing, T. Consi, F. J. Schoen, R. Langer, L. E. Freed, and G. Vunjak-Novakovic, "Functional assembly of engineered myocardium by electrical stimulation of cardiac myocytes cultured on scaffolds," dec 2004.

[33] Q. Zhang, J. Jiang, P. Han, Q. Yuan, J. Zhang, X. Zhang, Y. Xu, H. Cao, Q. Meng, L. Chen, T. Tian, X. Wang, P. Li, J. Hescheler, G. Ji, and Y. Ma, "Direct differentiation of atrial and ventricular myocytes from human embryonic stem cells by alternating retinoid signals," *Cell Research*, vol. 21, p. 579, nov 2010.

[34] C. E. Murry and G. Keller, "Differentiation of Embryonic Stem Cells to Clinically Relevant Populations: Lessons from Embryonic Development," *Cell*, vol. 132, pp. 661–680, feb 2008.

[35] X. Yang, M. Rodriguez, L. Pabon, K. A. Fischer, H. Reinecke, M. Regnier, N. J. Sniadecki, H. Ruohola-Baker, and C. E. Murry, "Tri-iodo-l-thyronine promotes the maturation of human cardiomyocytes-derived from induced pluripotent stem cells," *Journal of Molecular and Cellular Cardiology*, vol. 72, pp. 296 – 304, 2014.

[36] Y.-K. Lee, K.-M. Ng, Y.-C. Chan, W.-H. Lai, K.-W. Au, C.-Y. J. Ho, L.-Y. Wong, C.-P. Lau, H.-F. Tse, and C.-W. Siu, "Triiodothyronine promotes cardiac differentiation and maturation of embryonic stem cells via the classical genomic pathway.," *Molecular endocrinology (Baltimore, Md.)*, vol. 24, pp. 1728–1736, sep 2010.

[37] R. Troncoso, C. Ibarra, J. M. Vicencio, E. Jaimovich, and S. Lavandero, "New insights into igf-1 signaling in the heart," *Trends in Endocrinology & Metabolism*, vol. 25, no. 3, pp. 128 – 137, 2014.

[38] E. Ruoslahti, "RGD and other recognition sequences for integrins.," *Annual review of cell and developmental biology*, vol. 12, pp. 697–715, 1996.

[39] *Tissue Engineering*. 2nd ed., 2014.

[40] M. Maillet, J. H. van Berlo, and J. D. Molkentin, "Molecular basis of physiological heart growth: fundamental concepts and new players.," *Nature reviews. Molecular cell biology*, vol. 14, pp. 38–48, jan 2013.

[41] C. Mummery, D. W. van Oostwaard, P. Doevendans, R. Spijker, S. van den Brink, R. Hassink, M. van der Heyden, T. Opthof, M. Pera, A. B. de la Riviere, R. Passier, and L. Tertoolen, "Differentiation of human embryonic stem cells to cardiomyocytes," *Circulation*, vol. 107, no. 21, pp. 2733–2740, 2003.

[42] H. Shirahama, B. H. Lee, L. P. Tan, and N. J. Cho, "Precise tuning of facile one-pot gelatin methacryloyl (GelMA) synthesis," *Scientific Reports*, vol. 6, no. August, 2016.

[43] M. Djabourov and P. Papon, "Influence of thermal treatments on the structure and stability of gelatin gels," *Polymer*, vol. 24, no. 5, pp. 537 – 542, 1983.

[44] R. A. Bellantone, "What is G prime modulus in simple terms?," 2018.

[45] Unknown, "Basics of rheology."

[46] Unknown, "Young's Modulus or Storage Modulus."

[47] S. S. Datta, "Tutorial : Rheology of Soft Materials What Is Rheology?," *Soft Materials*.

[48] A. Chopra, E. Tabdanov, H. Patel, P. A. Janmey, and J. Y. Kresh, "Cardiac myocyte remodeling mediated by N-cadherin-dependent mechanosensing.," *American journal of physiology. Heart and circulatory physiology*, vol. 300, pp. H1252–66, apr 2011.

[49] I. Miccoli, F. Edler, H. Pfnür, and C. Tegenkamp, "The 100th anniversary of the four-point probe technique: The role of probe geometries in isotropic and anisotropic systems," *Journal of Physics Condensed Matter*, vol. 27, no. 22, 2015.

[50] Dojindo Molecular Technologies Inc, "Cell Staining Reagents," pp. 30–42, 2014.

[51] A. J. S. Ribeiro, Y.-S. Ang, J.-D. Fu, R. N. Rivas, T. M. A. Mohamed, G. C. Higgs, D. Srivastava, and B. L. Pruitt, "Contractility of single cardiomyocytes differentiated from pluripotent stem cells depends on physiological shape and substrate stiffness.," *Proceedings of the National Academy of Sciences of the United States of America*, vol. 112, pp. 12705–12710, oct 2015.

[52] H. Itoh, *Electrophysiological Simulation of Developmental Changes in Action Potentials of Cardiomyocytes*, pp. 75–88. 01 2013.

[53] N. Huebsch, P. Loskill, M. A. Mandegar, N. C. Marks, A. S. Sheehan, Z. Ma, A. Mathur, T. N. Nguyen, J. C. Yoo, L. M. Judge, C. I. Spencer, A. C. Chukka, C. R. Russell, P.-L. So, B. R. Conklin, and K. E. Healy, "Automated Video-Based Analysis of Contractility and Calcium Flux in Human-Induced Pluripotent Stem Cell-Derived Cardiomyocytes Cultured over Different Spatial Scales," *Tissue Engineering Part C: Methods*, vol. 21, no. 5, pp. 467–479, 2015.

[54] S. Taylor, K. Nadeau, M. Abbasi, C. Lachance, M. Nguyen, and J. Fenrich, "The ultimate qpcr experiment: Producing publication quality, reproducible data the first time," *Trends in Biotechnology*, 01 2019.

[55] S. Neidler, "What are the differences between PCR, RT-PCR, qPCR, and RT-qPCR?," 2017.

[56] D. C. Grahame, "The Electrical Double Layer and the Theory of Electrocapillarity.," *Chemical Reviews*, vol. 41, pp. 441–501, dec 1947.

[57] S. Westerlund and L. Ekstam, "Capacitor theory," *IEEE Transactions on Dielectrics and Electrical Insulation*, vol. 1, pp. 826–839, Oct 1994.

[58] Y. Wu, W. Koch, and K. Pratt, "Proposed new electrolytic conductivity primary standards for kcl solutions," *Journal of Research of the National Institute of Standards and Technology*, vol. 96, p. 191, 03 1991.

[59] M. T. Cole, V. Cientanni, and W. I. Milne, "Horizontal carbon nanotube alignment," *Nanoscale*, vol. 8, no. 35, pp. 15836–15844, 2016.

[60] J. Piquereau and R. Ventura-Clapier, "Maturation of Cardiac Energy Metabolism During Perinatal Development.," *Frontiers in physiology*, vol. 9, p. 959, 2018.

[61] C. Robertson, D. D. Tran, and S. C. George, "Concise review: maturation phases of human pluripotent stem cell-derived cardiomyocytes.," *Stem cells (Dayton, Ohio)*, vol. 31, pp. 829–837, may 2013.

[62] J. Wang, C. Cui, H. Nan, Y. Yu, Y. Xiao, E. Poon, G. Yang, X. Wang, C. Wang, L. Li, K. R. Boheler, X. Ma, X. Cheng, Z. Ni, and M. Chen, "Graphene Sheet-Induced Global Maturation of Cardiomyocytes Derived from Human Induced Pluripotent Stem Cells," *ACS Applied Materials & Interfaces*, vol. 9, no. 31, pp. 25929–25940, 2017.